UCLouvain

Faculté de pharmacie
et des sciences biomédicales

Unraveling the role of Slc13A3 and Slc13A5 in acute myeloid leukemia

Autrice : Justine Berny
Promoteur : Nick van Gastel
Superviseur : Lotfi Laaouimir
Lecteurs : Pierre Sonveaux and Pierre van der Bruggen
Année académique 2025-2026
Master en sciences biomédicales, option approfondie

Acknowledgement

I would like to first of all thank Nick van Gastel for welcoming me in the MeMi lab and this amazing team during my internship. I am so happy I got to share this year with my colleagues: Dr Nithya Balasundaram, Dr Ayşegül Erdem, the future doctors Hernan Andres Tirado Cardenas, Célina Nielsen, Torben Roy, Célia Sergi, Aymane Hadj M'Hand and the lab technicians Ipek Can and Fleur Leguay.

To Lotfi Laaouimir, شكرًا for the patience, the attentiveness, the guidance. I will forever be grateful that I got to work with you. I leave this place knowing I got the best teacher I could have ever asked for and a chaotic, talented friend.

Merci à mes parents qui ont toujours cru en moi malgré une multitude de bas et mes années d'étude chaotique.

Merci à notre petit groupe de master "Un ptit verre ? (de citronnade)" qui m'a permis d'avoir une véritable bouffée d'air frais les lundis. Merci pour ces échanges et notre amitié.

Merci à mon intemporel groupe "Taffe tes morts au golf", les copines qui ont été là toutes ces années pour les blocus mais surtout nos meilleures parties de mini-golf sur discord. Hâte de vous mettre un zanyball.

Merci au PHOS lab qui était un refuge à mes moindres sautes d'humeur.

TABLE OF CONTENT

Abbreviations

2-HG	2-hydroxyglutarate
7-AAD	7-aminoactinomycin D
αKG	α-ketoglutarate
Acly	ATP-dependent citrate lyase
AML	acute myeloid leukemia
AMP	adenosine monophosphate
Asn	asparagine
ASNS	asparagine synthetase
Asp	aspartate
ATP	adenosine triphosphate
BCAA	branched-chained amino acids
BMSC	bone marrow stromal cells
CoA	Coenzyme A
cDNA	complementary DNA
CHIP	clonal haematopoiesis of indeterminate potential
CTP	cytosine triphosphate
CP	carbamoyl phosphate
CPS	carbamoyl phosphate synthetase
Cys	cysteine
dFBS	dialyzed FBS
DNA	deoxyribonucleic acid
DNMT3A	DNA methyltransferase 3A
dNTP	deoxyribonucleotide triphosphate
DOT1L	disruptor of telomeric silencing 1-like
ETC	electron transport chain
FACS	Fluorescence-activated cell sorting
$FADH_2$	Reduced flavin adenine dinucleotide
FBS	foetal bovine serum
FLT3	FMS-like tyrosine kinase 3
GC/MS	Gas chromatography / mass spectrometry
GFAT	glutamine-fructose-6-phosphate transaminase
Gln	glutamine
GLS	glutaminase
Glu	glutamate
GLUD	glutamate dehydrogenase
GMP	guanine monophosphate
GOT	glutamic-oxaloacetic transaminase
GPT2	glutamic-pyruvic transaminase 2
GSH	glutathione
HSC	hematopoietic stem cell
KD	knock-down
KMT2A	lysine methyltransferase 2A
iCT	induction chemotherapy
ITD	internal tandem duplication
IDH	isocitrate dehydrogenase
L-BSO	L-buthionine sulfoximine
LDH	lactate dehydrogenase
LPC	lymphoid progenitor cells
LT	long term
mAML	murine acute myeloid leukemia
MLL	mixed lineage leukemia
MPC	myeloid progenitor cells
NAC	N-acetylcysteine
NADH	reduced nicotinamide adenine dinucleotide

NALA	N-acetyl-L-aspartate
NH_3	ammonia
NK	Natural killer
NPM1	Nucleophosmin 1
PPAT	phosphoribosyl pyrophosphate amidotransferase
PRA	5-phosphoribosyl-1-amine
QC	quality control
NADPH	reduced nicotinamide adenine dinucleotide phosphate
RNA	ribonucleic acid
ROS	reactive oxygen species
RPM	revolutions per minute
RT-qPCR	real time-quantitative polymerase chain reaction
sh	short hairpin
SLC	solute carrier
TCA (cycle)	tricarboxylic acid (cycle)
UTP	uridine triphosphate
UDP- Glc-NAc	uridine diphosphate N-acetylglucosamine

Summary

Acute myeloid leukemia (AML) is an aggressive hematopoietic malignancy characterized by the uncontrolled proliferation of undifferentiated myeloid cells. Previous work from our laboratory has shown that bone marrow stromal cells (BMSCs) further protect AML cells by stimulating their glutamine and aspartate metabolism. Interestingly BMSCs also release TCA cycle metabolites into their microenvironment. However, whether AML cells directly utilize these BMSC-derived TCA cycle metabolites remains unknown. To determine whether AML cells are capable of taking up exogenous TCA cycle metabolites, we first assessed the expression of TCA cycle metabolite transporters. We found that AML cells express both Slc13A3 and Slc13A5. We then performed a genetic knockdown of Slc13A5 in murine AML cells and exposed them to various metabolic stress conditions. Notably, Slc13A5-deficient AML cells cultured in glutamine-free media exhibited significantly increased cell death compared to control cells, suggesting that metabolites transported via Slc13A5 are critical for AML cell survival under conditions of limited glutamine availability. Additionally, Slc13A3 expression is strongly upregulated under glutamine-free conditions, suggesting increased dependence on transporter-mediated metabolite uptake. Among potential substrates, adding α-ketoglutarate restored the viability of AML cells in glutamine-free media. α-ketoglutarate can be used to generate citrate, which is then converted into cytosolic acetyl-CoA for lipid synthesis or protein acetylation. Interestingly supplementing with acetate, partially rescued the Slc13A5-deficient cells' viability upon exposure to lower glutamine levels. This shows that the increased mortality of Slc13A5-deficient cells in glutamine-free conditions might result from a critical shortage of the acetyl-CoA pool in the cytosol. In conclusion, this project identifies Slc13A5 as a key metabolic regulator that supports AML cell survival under glutamine-deprived conditions by promoting metabolic flexibility. These findings provide new mechanistic insight into how AML cells adapt to nutrient stress and highlight Slc13A5 as a potential therapeutic target. Combining Slc13A5 inhibition with glutamine-targeted therapies may help overcome metabolic resistance and improve treatment efficacy in AML.

Résumé

La leucémie myéloïde aiguë (LMA) est une tumeur maligne hématopoïétique agressive, caractérisée par la prolifération incontrôlée de cellules myéloïdes indifférenciées. Des travaux antérieurs de notre laboratoire ont montré que les cellules stromales de la moelle osseuse (CSMO) protègent les cellules de LMA en stimulant leur métabolisme de la glutamine et de l'aspartate. Curieusement, les CSMO libèrent également des métabolites du cycle de Krebs dans leur microenvironnement. Cependant, on ignore si les cellules de LMA utilisent directement ces métabolites dérivés des CSMO. Pour déterminer si les cellules de LMA captent des métabolites exogènes du cycle de Krebs, nous avons évalué l'expression de leurs transporteurs. Nous avons constaté que les cellules de LMA expriment Slc13A3 et Slc13A5. Nous avons ensuite procédé à un knockdown génétique de Slc13A5 dans des cellules de LMA murines exposées à diverses conditions de stress métabolique. Notamment, les cellules de LMA déficientes en Slc13A5 cultivées dans un milieu sans glutamine ont présenté une mortalité cellulaire significativement accrue par rapport aux cellules contrôles. Cela suggère que les métabolites transportés via Slc13A5 sont essentiels à la survie des cellules de LMA sous disponibilité limitée en glutamine. De plus, l'expression de Slc13A3 est fortement régulée à la hausse sans glutamine, suggérant une dépendance accrue envers l'absorption de métabolites médiée par les transporteurs. Parmi les substrats potentiels, l'ajout d' α-cétoglutarate a restauré la viabilité des cellules de LMA dans un milieu sans glutamine. L' α-cétoglutarate peut générer du citrate, qui est ensuite converti en acétyl-CoA cytosolique pour la synthèse des lipides ou l'acétylation des protéines. De plus, une supplémentation en acétate a partiellement rétabli la viabilité des cellules déficientes en Slc13A5 lors de l'exposition à de faibles taux de glutamine. Cela démontre que la mortalité accrue des cellules déficientes en Slc13A5 sans glutamine pourrait résulter d'une pénurie critique d'acétyl-CoA dans le cytosol. En conclusion, ce projet identifie Slc13A5 comme un régulateur métabolique clé soutenant la survie des cellules de LMA en favorisant la flexibilité métabolique. Ces résultats apportent un éclairage mécanistique sur l'adaptation des cellules de LMA au stress nutritionnel et désignent Slc13A5 comme une cible thérapeutique potentielle. Combiner l'inhibition de Slc13A5 avec des thérapies ciblant la glutamine pourrait aider à surmonter la résistance métabolique et améliorer l'efficacité du traitement.

Introduction

Hematopoiesis

Hematopoietic stem cells (HSCs) represent the earliest progenitor cells within the hematopoietic lineage. Like all stem cells, HSCs possess the capacity for self-renewal and multipotent differentiation, enabling them to give rise to various blood cell types. A defining feature of a subset of HSCs, known as long-term hematopoietic stem cells (LT-HSCs), is their state of quiescence. This dormancy limits cellular proliferation, thereby reducing the risk of mutation accumulation and contributing to the long-term maintenance of the stem cell pool within the bone marrow niche.

In this microenvironment, the HSCs will either differentiate into myeloid progenitor cells (MPCs) or lymphoid progenitor cells (LPCs). LPCs give rise to T cells, B cells, NK cells and plasma cells, while MPCs produce megakaryocytes (which produce platelets), eosinophils, basophils, erythrocytes, monocytes (which differentiate into dendritic cells or macrophages) and neutrophils.

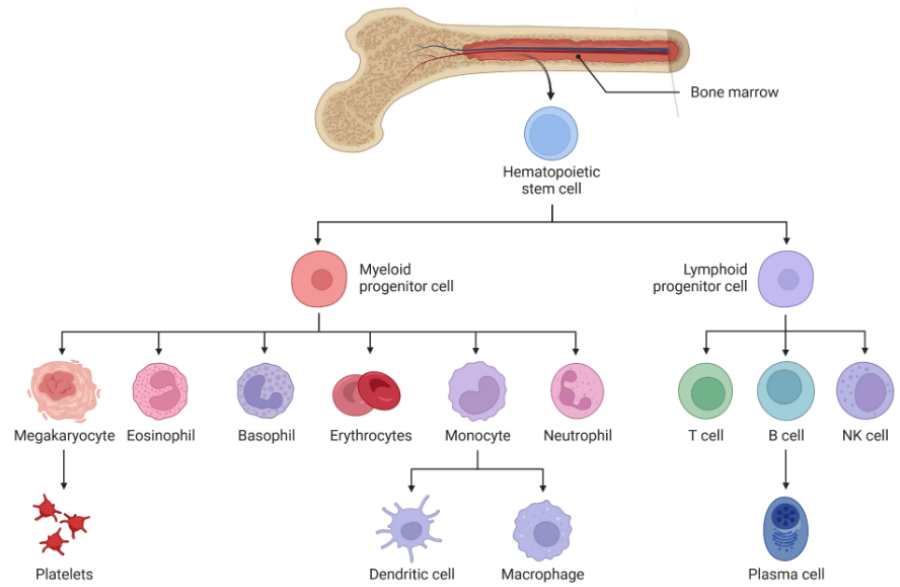

Figure 1: Hematopoiesis (Akiko Iwasaki on BioRender)

Pre-leukemic transformation of HSCs

In their lifespan, HSCs undergo numerous rounds of replication during which they can acquire somatic mutations. While most mutations are inconsequential, some can confer an advantage, either by enhancing proliferative capacity or altering differentiation potential. When such a mutation leads to the expansion of a haematopoietic clone in the absence of overt malignancy, the condition is referred to as clonal hematopoiesis of indeterminate potential (CHIP) (Corces et al., 2017).

CHIP cells, having an advantage, will gradually expand in the bone marrow, providing a fertile ground to accumulate additional mutations and evolve into hematopoietic malignancies, such as acute myeloid leukemia. The most frequent mutation observed in CHIP cells is in the *DNMT3A* gene, which is one of the most prevalent mutations in acute myeloid leukemia as well (Corces et al., 2017).

Acute myeloid leukemia

AML is a cancerous disease in which cells of the myeloid lineage of haematopoiesis acquire mutations, proliferate abnormally and do not differentiate properly. The disease often presents the same mutated genes: *NPM1*, *DNMT3A*, *FLT3*, and *MLL* rearrangements (Döhner et al., 2015).

First, there is *FLT3* (around 30% of AMLs) (Kiyoi et al., 2020), FMS-like tyrosine kinase, a receptor which binds *FLT3* ligand. The most common mutation is called *FLT3-ITD* (internal tandem duplication), causing a constitutive activation of the receptor. This leads to the activation of the *Ras* and *Stat5* pathways, which will upregulate cell proliferation (Macečková et al., 2024).

Next is *NPM1*, or nucleophosmin (30% of AMLs) (Döhner et al., 2015); a phosphoprotein found in nucleoli, cytoplasm and nucleoplasm. It intervenes in many processes, for instance: centrosome duplication, cell cycle control (Okuda, 2002), DNA replication and repair (Scott & Oeffinger, 2016). In Kunchala et al., (2018), it is explained that most of the time, the mutation of the gene results in a

displacement of the protein to the cytoplasm, preventing it from accomplishing its function in the nucleoli.

The third most encountered mutated gene is *DNMT3A* (20% of AMLs) (Döhner et al., 2015). This is a DNA methyltransferase targeting cytosine in CpG islands. When these islands are methylated by *DNMT3A*, the transcription of the gene related to it is repressed. However when *DNMT3A* is mutated and lost, it leads to DNA hypomethylation, resulting in loose chromatin structures, failed inactivation of X chromosome, as well as an inefficient imprinting control (Robertson et al., 1999; W. Zhang & Xu, 2017).

It is found especially in pediatric AML and means Mixed Lineage Leukemia (MLL; encoded by the *Kmt2a* gene) rearrangements. It results from chromosomal translocations. The most studied rearrangement is *MLL-AF9*, a fusion gene resulting from a translocation between chromosomes 9 and 11. Normally, Kmt2a is recruited by the Menin-LEDGF complex, allowing the Kmt2a-C terminal protein to catalyze the H3K4 methylation, activating the transcription of *HOXA9* and *MEIS1* (Figure 1A). In leukemic cells, the Kmt2a-C terminal part of the protein is replaced by a fusion protein (here AF9) and binds to the DOT1L complex, altering the transcription regulation profile. The recruitment of the DOT1L complex then leads to a persistent and uncontrolled transcription of *HOXA9* and its co-factor *MEIS1*, which drive leukemogenesis through diverse mechanisms. (Figure 1B) (Winters & Bernt, 2017; Zehtabcheh et al., 2025)

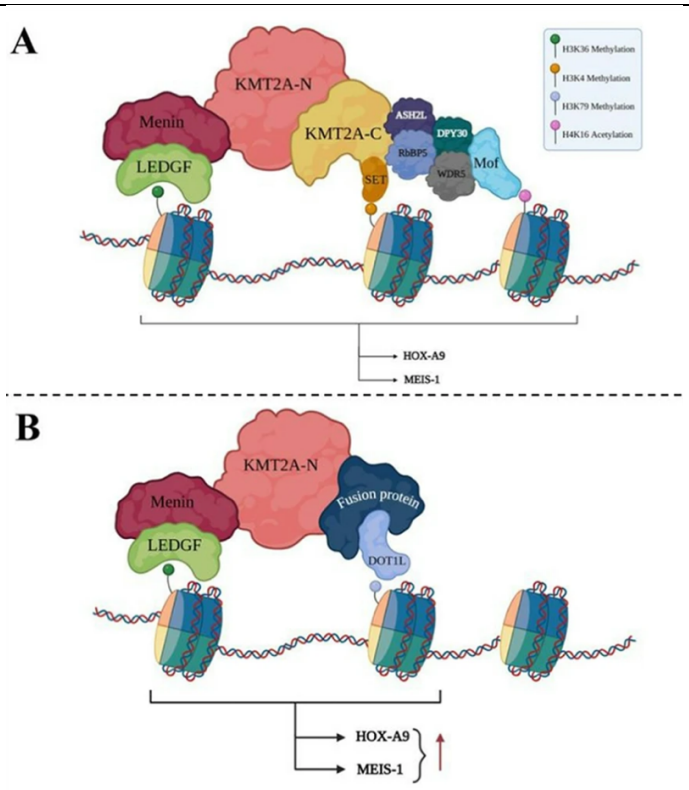

Figure 5: Regulation by Kmt2a and its rearrangements of *HOXA9* and *MEIS1* expression. (A) Normal *Kmt2a* function. (B) Leukemogenic *Kmt2a* rearrangements. (adapted from Zehtabcheh et al., 2025)

Leukemic metabolism

In 2011, Hanahan and Weinberg established the 10 hallmarks of cancer, which represent key biological capabilities acquired during the multistep development of human tumours. These hallmarks are characteristics which differentiate cancer cells from healthy cells and allow cells to grow without being eliminated: sustaining proliferative signaling, evading growth suppressors, avoiding immune destruction, enabling replicative immortality, tumour-promoting inflammation, activating tissue invasion and metastasis, inducing angiogenesis, provoking mutations and genome instability, resisting cell death, and deregulated cellular metabolism. With regards

to the current project, we focus here on the most common metabolic alterations found in AML.

Glycolytic pathway

Upon import into the cell, glucose enters the glycolytic pathway, undergoing a series of enzymatic reactions to generate pyruvate. In healthy cells under normoxic conditions, pyruvate is transported into the mitochondria and enters the tricarboxylic acid (TCA) cycle for oxidative energy production. Under hypoxic conditions, however, pyruvate is instead used to generate lactate by an enzyme called lactate dehydrogenase (LDH).

In cancer cells, even if the environment is abundant in oxygen, there is a switch from oxidative to glycolytic metabolism (i.e. Warburg effect), meaning that once the pyruvate is produced by glycolysis, it is converted into lactate through LDH enzymes, catalyzing the transformation of NADH into NAD^+, to sustain glycolysis (Liberti & Locasale, 2016).

As pyruvate is no longer fueling the TCA cycle, AML cells find other means to maintain the activity of the TCA cycle. One way is by using glutamine to generate α-ketoglutarate which can be incorporated to the TCA cycle (Willems et al., 2013).

In AML, a known change is the change of localization of Hk2 to the nucleus where it support the stemness of the cells, and regulates gene expression (Thomas et al., 2022).

Mitochondrial metabolism

After the generation of pyruvate, it is converted into acetyl-CoA which is fueling the TCA cycle. The TCA cycle is a generator of NADH, ATP and $FADH_2$ which are redirected to the electron transport chain (ETC), a group of proteins located in the inner membrane of the mitochondria, consisting of a succession of redox reactions, going from complex I to V. This process is what is known as oxidative phosphorylation, the fifth and last complex of the ETC is the ATP synthase, it uses

the proton gradient generated by the other complexes when turning NADH and $FADH_2$ into NAD^+ and FAD^+ to fuel the synthesis of ATP (Mesbahi et al., 2022). In AML, it is often observed that their metabolism switch from glycolytic to oxidative metabolism, leading to a high dependency on mitochondria. It was also shown that mitochondria were compromised in AML due to the mutations of Idh enzymes, generating 2-hydroxyglutarate, an onco-metabolite (Panina et al., 2021).

Amino acid synthesis

Out of the 20 amino acids, 9 are considered as essential and must be obtained through diet. However, in certain circumstances, some amino acids, considered as non-essential, may become essential, they are called conditionally essential amino acids. As cancer cells reprogram their metabolism to proliferate more rapidly, they stop the biosynthesis of certain non-essential amino acids, increasing their reliance on exogenous sources.

Cancerous cells become dependent on glutamine to fuel their TCA cycle, which is an important pathway to fuel fatty acids synthesis, pyrimidine synthesis, purine synthesis, glutathione synthesis, and the maintenance of redox balance through the reduction of reactive oxygen species (ROS) (Choi & Coloff, 2019).

In addition to glutamine, branched-chain amino acids (BCAA: leucine, isoleucine, and valine) also play pivotal roles in LSCs metabolism. Altered BCAA catabolism has been implicated in enhancing tumour progression and cancer cell survival (Xu et al., 2023). A key enzyme in this process is branched-chain amino acid transaminase 1 (BCAT1), it is frequently upregulated in multiple tumour types, including AML, and is involved in the maintenance of the stemness of the cells.

Nucleotide synthesis

Nucleotide synthesis is usually following the salvage pathway where nucleotides are "recycled", however in cancers there is a switch from the salvage pathway to the *de novo* pathway despite it being more ATP costing than the former. We know that

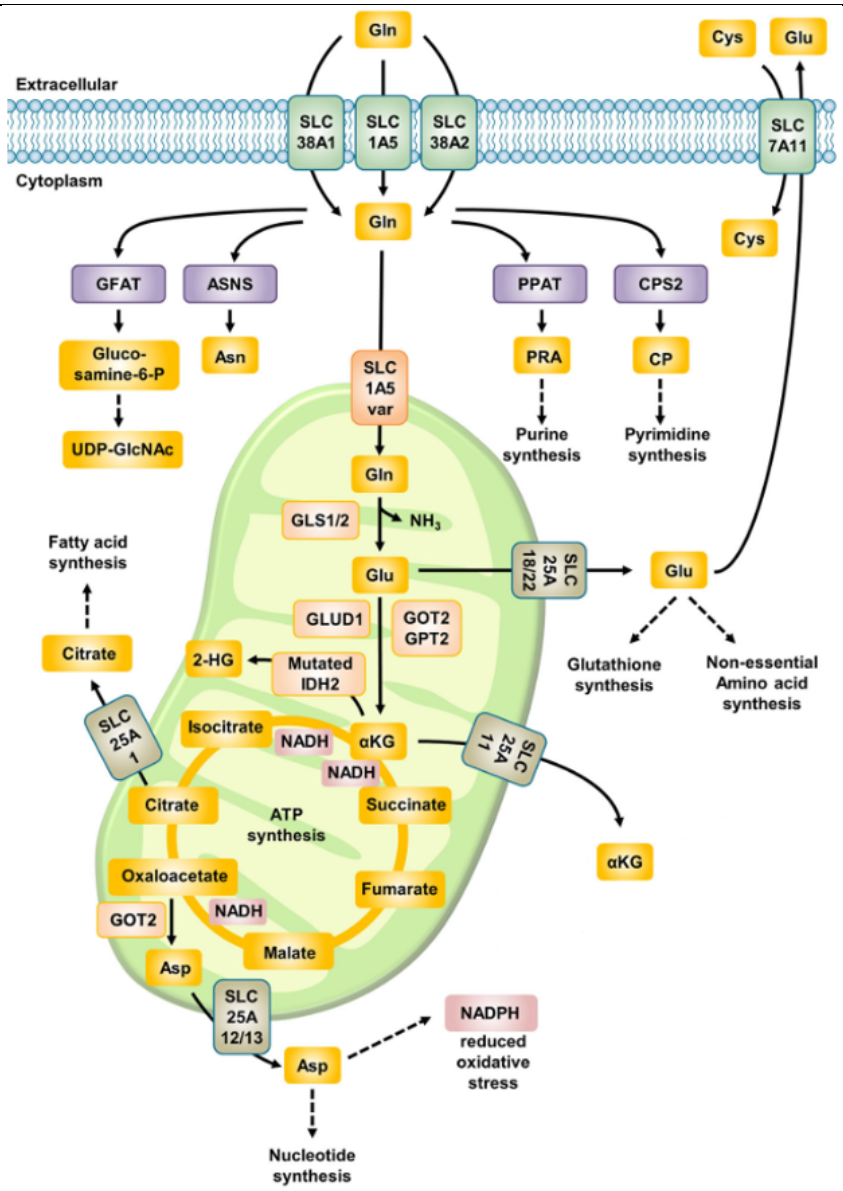

Figure 2: Glutamine metabolic pathways. (adapted from Yoo et al., 2020)

proliferative cells rely highly on the nucleotides synthesis to be able to replicate their DNA by using UTP, CTP, AMP and GMP (see figure 3), explaining that cancerous cells, uncontrollably proliferative, are greatly relying on this pathway. Additionally, glutamine is a building block for both purine and pyrimidine synthesis (Tran et al., 2024).

Fatty acid metabolism

Usually, fatty acids are synthesized by acetyl-CoA which is generated in the cytosol from citrate exported from the mitochondria. In leukemic cells, as glutamine-derived carbon supports TCA cycle intermediates, glutamine also indirectly fuels fatty acid synthesis, similarly to its role in amino acid and nucleotide metabolism, see figure 2. (Currie et al., 2013)

AML relies as well on β-oxidation of fatty acids as a source for energy that they require for their high proliferation rate, but it has also been shown to fuel drug resistance (Farge et al., 2017). However, mutations in the enzymes of β-oxidation are not recurrent in cancer despite the increase of the mechanism (Ma et al., 2018; Kreitz et al., 2019).

Context

In a previous study from our lab (van Gastel et al., 2020), it was demonstrated that AML cells are protected from chemotherapy when co-cultured with bone marrow stromal cells (BMSCs). This protective effect is mediated by the release of aspartate from BMSCs, which AML cells utilize to support nucleotide synthesis. Interestingly, it was also observed that BMSCs secrete additional TCA cycle metabolites into the microenvironment (Figure 4). However, it remains unclear whether AML cells take up and metabolize these BMSC-derived TCA metabolites.

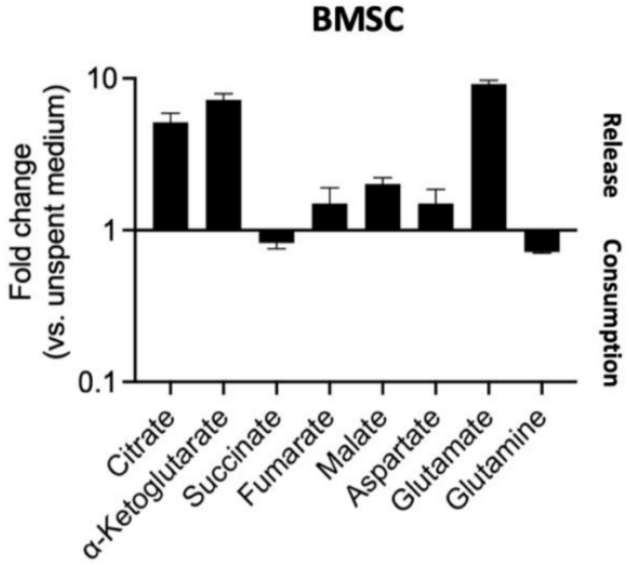

Figure 3: Quantification of TCA metabolites released and consumed by bone marrow stromal cells by LC-MS. (Unpublished data)

As the levels of the BMSC-secreted citrate and α-ketoglutarate are higher than aspartate a hypothesis was established that the AML cells take up citrate/α-ketoglutarate to fuel their metabolism and support their growth. However, when the cells were cultured in the presence of increasing concentrations of citrate, they underwent apoptosis, while adding α-ketoglutarate had no effect, negating therefore the hypothesis. Interestingly AML cells do express TCA cycle metabolite transporters, mainly SLC13A3 and SLC13A5 (which can both induce the uptake of citrate and α-ketoglutarate). Whether these transporters allow AML cells to take up

other substrates, and under which conditions they become important, remains unknown.

Of note, the expression of plasma membrane transporters for TCA cycle metabolites (*Slc13A3*, *Slc13A5*) in AML cells is transiently reduced following chemotherapy exposure in vivo. At the moment of maximal response after induction chemotherapy (iCT, a combination of doxorubicin and cytarabine), the expression of both transporters is significantly decreased, but the expression is reverted to normal after relapse (Figure 5). There is no data for the *Slc13A2* as the gene is not expressed in the mAML cells utilized.

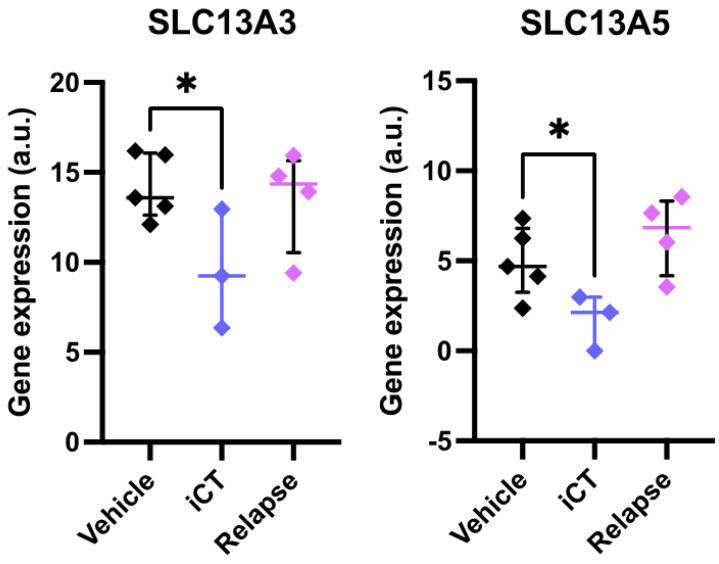

Figure 4: Gene expression of Slc13A3 and Slc13A5 transporters in vehicle, iCT or relapse in MLL-AF9 AML cells, measured by RNA sequencing. (van Gastel et al., 2020)

Solute carriers 13A2, 13A3 and 13A5

The *Slc13A* transporters are a family of transporters that carries solutes (di-/tri-carboxylates or sulfates) with 2 to 4 sodium ions from the extracellular environment into the cytoplasm. There are 5 family members: *Slc13A1*, *Slc13A2*, *Slc13A3*, *Slc13A4* and *Slc13A5*.

However, as we are focusing on the role of TCA cycle metabolites and given that *Slc13A2* is not expressed in our cells, we will only discuss the functions of *Slc13A3* and *Slc13A5* in detail.

	Predominant physiological substrates	Tissue distribution and cellular/subcellular expression
Slc13A1	Sulfate Selenate Thiosulfate	Kidney, proximal tubular cells, brush border membrane
Slc13A2	Succinate Citrate α-ketoglutarate	Kidney, intestine, brush border membrane
Slc13A3	Succinate, citrate, α-ketoglutarate, NALA, glutathione, itaconate, glutarate and its derivatives	Kidney, proximal tubule, basolateral membrane, liver, pancreas, brain, placenta
Slc13A4	Sulfate Oxyanions selenium and chromium	Placenta, tonsillar high endothelial venules, testis, heart
Slc13A5	Citrate Succinate Pyruvate	Liver, brain, testis

Table 1: SLC13 – the human Na^+-sulfate/di- and tri-carboxylate cotransporter family.

Slc13A2

Also known as NADC1, the Slc13A2 transporter is localized in kidney, intestine and brush border membrane. It transports TCA cycle metabolites such as succinate, citrate and α-ketoglutarate.

Slc13A3

Also known as NaDC3, the Slc13A3 transporter is mainly localized in the brain, the choroid plexus, the kidneys, the liver and the eyes. It transports tricarboxylates like succinate, α-ketoglutarate, fumarate, malate, dimethyl-succinate and citrate (Bergeron et al., 2013), as well as itaconate, a citrate-derived metabolite (Haase & Frezza, 2024) and glutathione (Zhao et al., 2024).

Interestingly, it is showed in Z. Zhang et al., (2020) that the overexpression of *Slc13A3* might suppress leukemogenesis to a certain extent and is linked to ROS levels.

There has been report of a few cases of leukoencephalopathy caused by mutations of the Slc13A3 gene. One of them is called acute reversible leukoencephalopathy with increased urinary α-ketoglutarate and is characterized by an acute neurologic involvement, often precipitated by febrile illness.

Slc13A5

Also known as NaCT, the Slc13A5 transporter is broadly found in the brain but is also present in the liver and testis. It has a high affinity towards citrate mainly, but it can also transport succinate and pyruvate with a lower affinity. The cotransporter is coupled to sodium; to make one substrate get into the cytoplasm, the transporter needs 4 cations of sodium (Bergeron et al., 2013).

The Slc13A5 cotransporter is important in the brain, it is found in neuronal membrane. The outcome of a *Slc13A5*-deficiency in the neurons is an epileptic encephalopathy. Patients have early onset seizures, associated with a developmental delay and intellectual disability (Thevenon et al., 2014).

Slc13A5 is intricately linked to citrate and its intracellular effects since this is its primary transported substrate. In Kumar et al. (2021), it has already been shown that, in Huh7 cells, citrate supplementation is an option to rescue cell viability in case of glutamine deprivation.

Citrate and acetyl-CoA metabolism

Citrate, or citric acid, is an integral metabolite of cell metabolism. Crucial part of the TCA cycle, it is also a precursor of several important molecules as acetyl-CoA, oxaloacetate and itaconate. Acetyl-CoA is a key metabolite as it is a precursor of the fatty acid synthesis and a precursor of acetylation, making it a crucial regulator of DNA transcription and protein modification, which can play a crucial role in the increased proliferation, dissipation and chemoresistance of cancerous cells (Cai et al., 2011; Hao et al., 2022).

Objectives

During my Master thesis research, I focus on studying the role of the Slc13A3 and Slc13A5 transporters in AML. The main aim of this study is to assess the survival of *Slc13A5*-deficient AML cells when exposed to different conditions to identify the potential advantages/disadvantages that this transporter confers.

Methods

Cell model

In this research, only murine AML cell line bearing the MLL-AF9 rearrangement were used. This cell line was established by crossing MLL-AF9 knock in mice with mice expressing GFP (under the control of the ubiquitin promoter) and luciferase (under the control of ß-actin promoter) (van Gastel et al., 2020).

Cell culture

The mouse AML cell lines are cultured in RPMI1640 medium (Sigma-Aldrich) supplemented with 10% Foetal Bovine Serum (FBS), 1% penicillin-streptomycin (Pen-Strep) (final concentration of 0,1mg/mL), 2mM glutamine, 10ng/ml of interleukin-3 (IL-3), 10ng/ml of interleukin-6 (IL-6) and 20ng/ml of stem cell factor (SCF). As the mAML cell lines contain a short hairpin RNA, they are treated with puromycin (1mg/mL) for positive selection. Cells are incubated at 37°C, 5% CO_2 and 21% O_2.

When passaged, the suspension cells are in a T25 flask and the flask is tapped by hand on the side several times, allowing the cells to naturally detach from the bottom of the flask. The cells are harvested and put in a 50mL tube, to be spun down at 500g for 5 minutes in a centrifuge at room temperature. The supernatant is discarded, and the pellet of cells is resuspended in 1mL of media. An 1,5mL microcentrifuge tube is prepared on the side with 10µL of trypan blue (30%). After resuspension of the cells, 10µL of cells is added to the 1,5mL microcentrifuge tube and mixed to trypan blue, 10µL of this solution is added in a counting slide. The number of cells is acquired with the Cell counter Countess (ThermoFischer).

For the weekend, the cells are seeded differently depending on which cell line it is as their proliferation speed is different. shQC are seeded at a concentration of 5 000

cells per cm^2, 4 500 cells per cm^2 for shSlc13A5 (1) and 4 000 cells per cm^2 for shSlc13A5 (2). Each cell line is seeded in 10mL of media in a T25 flask.

ImageXpress PICO

Image Xpress PICO is an automated cell imaging system. 5 000 cells were seeded in wells in a 96 well plate in 200µL of RPMI. Pictures were automatically taken every 6 hours for a total period of 96 hours. GFP positive cells i.e. viable AML cells were automatically counted using a cell counting filter in CellReporter Xpress software.

RNA extraction

1 000 000 mAML cells were harvested and washed twice with 1mL of PBS and resuspended into 1mL of Trizol. Samples can be stored at -80°C or we can proceed with chloroform. 0,2mL of chloroform for 1mL of Trizol were added, each sample is vortexed for 10 seconds then incubated 10 minutes at room temperature. Samples are then centrifuged 15 minutes at 12 000g and 4°C, creating 3 phases, the upper phase is taken out and put into a new 1,5mL microcentrifuge tube. To this new 1,5mL microcentrifuge tube, 0,5mL of isopropanol were added, vortexed for 10 seconds, incubated for 10 minutes at room temperature then centrifuged 8 minutes, at 12 000g and 4°C, it creates a gel-like pellet, corresponding to the precipitation of mRNA. 1,1mL of a solution of ammonium acetate (100µL of 4M ammonium acetate, 500µL DNAse and RNAse free water and 500µL isopropanol) is added and vortexed for 10 seconds, samples are incubated 20 minutes at room temperature. Afterwards, samples were centrifuged at 12 000g at room temperature for 15 minutes. The supernatant was then discarded and 1mL of ice-cold 75% ethanol was added, the sample was vortexed 10 seconds and centrifuged 5 minutes at 12 000g at 4°C. Carefully the ethanol was discarded by flipping the tube upside down and by letting the ethanol flow out on a tissue, the pellet was then left to air-dry until every droplet of ethanol disappeared. To end, 20µL of DNAse and RNAse free water was then added, and the tube was set on a heat block at 55°C for 5 minutes, vortexed for 10

seconds and put back for 5 minutes on a heat block at 55°C. For each sample, mRNA is quantified to the NanoDrop. The quality of each sample is evaluated by the 260/280 and 260/230 ratios. The 260/280 ratio corresponds to the protein contamination and is ideally around 2 to 2,2. The 260/230 ratio corresponds to the salt contamination and is ideally between 2 and 2,2, it is improved by the ammonium acetate step which precipitates salt as to get rid of contamination.

cDNA synthesis

To synthesize 20µL of cDNA for one sample, a master mix was made and composed of 4µL of reaction buffer (250 mM Tris-HCl (pH 8.3), 250 mM KCl, 20 mM MgCl2, 50 mM DTT), 2µL of deoxynucleotide triphosphate (dNTP), 1µL of Reverse Transcriptase enzyme, 1µL of RiboLock and 1µL of Random Primers for a total of 9µL. On the side, 11µL of a 250-100µg concentration of RNA was made. In a PCR tube, 9µL of the master MIX and 11µL of the RNA solution were added, centrifuged in the mini centrifuge. The PCR tube was then put into the PCR machine, and the cDNA program provided by the protocol was run (*RevertAid First Strand cDNA Synthesis Kit 100 Reactions | Buy Online | Thermo Scientific™*, s. d.).

RT-qPCR

For the qPCR, a master MIX was made and composed of 5µL of either SYBRGreen buffer or Taq-Man buffer (depending on the primers), 1µL of primers (corresponding to the gene of interest) and 3µL of RNAse and DNAse free water. In a qPCR plate, 9µL of master MIX were added at the bottom of the well then 1µL of cDNA was added to the top side of the well. The qPCR plate was then covered with a plastic seal, centrifuged for 1 minute at 300g and put into the Quantstudio 1 Real Time PCR System and was run under the "Comparative Ct with Melt" program. Before every qPCR, a template was designed on the ThermoFisher Scientific website.

Once the RT-qPCR is done, the data is recuperated. For each well, a value corresponds to Cq, the number of cycles needed to be detected by the machine. Each well was normalized to the expression of ß-actin. We subtracted each ΔCq value to that average Cq. Lastly, the gene expression relative to actin, equal to one, is calculated with $2^{-\Delta\Delta Ct}$.

Viability assay: glucose- or glutamine-depleted media in 48-well plate

In a 48 well plate, 50 000 mAML cells were seeded and cultured in 0,5mL of either glucose-free medium or glutamine-free medium for 24 hours. To create the different media, Agilent Seahorse XF RPMI Medium was used where 10% FBS, 1% pen-strep, 2mM glutamine (or not), 11,1mM of glucose (or not), 10ng/ml of interleukin-3 (IL-3), 10ng/ml of interleukin-6 (IL-6) and 20ng/ml of stem cell factor (SCF) were all added to respect the proportion of the complete RPMI medium used for the usual cell culture. This Agilent Seahorse XF RPMI Medium was used because of its lack of glucose.

After 24 hours, the cells were harvested and put into 5mL round bottom polystyrene tubes. The tubes were centrifuged, 5 minutes at 500g, and the supernatant was taken out, the cells were washed with 1mL of PBS, centrifuged 5 minutes at 500g and the supernatant was discarded again. The cells were then incubated with 100µL of a mix of 100µL of AnnexinV buffer, 0,5µL of AnnexinV and 1µL of 7-AAD, each 5mL round bottom polystyrene tubes was then vortexed. After incubating 10 minutes in the dark at room temperature, 100µL PBS were added and the samples were acquired and analyzed using a FACS Verse.

In a proapoptotic state, the cell membrane changes, and phosphatidylserine flips from the inner membrane to the extern membrane. AnnexinV will bind to phosphatidylserine.

7-AAD is an intercalant agent, as the cell becomes apoptotic, the membrane

becomes permeable and 7-AAD can across the plasmic membrane and introduce itself into the DNA.

Viability assay: rescue attempts

In a 96 well plate, each cell line was plated in normal media and glutamine-free media and treatment were added.

24 hours later, the plate was spun down 5 minutes at 500g, the supernatant was discarded and 50µL of 0,5% trypsin was added to each well. The plate was incubated for 2 minutes at 37°C, then 100µL of PBS were added to each well. With a multichannel pipette, up and downs were done and the cells were taken out and added in the FACS 96 well plate. The plate was once again spun down at 500g for 5 minutes, the supernatant was then discarded. 50µL of a mix of 50µL of AnnexinV buffer, 0,5µL of AnnexinV and 1µL of 7-AAD was added and the plate incubated for 10 minutes at room temperature in the dark. After 10 minutes, 100µL of PBS were added to each well. 10 000 events were then acquired with the FACSVerse.

Treatments preparation

For N-acetylcysteine, succinate, sodium pyruvate, glutarate, lysine-monohydrate chloride, tryptophan and sodium acetate: All these metabolites were powders. For each, a solution of 100mM was prepared in PBS, the pH was measured and adjusted with HCl (1M) or NaOH (10M), when necessary. The concentrations used were 1mM, 2,5mM and 5mM.

For dimethyl-itaconate and dimethyl-2-oxoglutarate: these metabolites are in solution at 7M and 6,9M respectively. Intermediate stocks were prepared at 100mM each. pH was measured and adjusted with HCl (1M) or NaOH (10M), when necessary. Dimethyl-itaconate was used at 2,5mM and 5mM, dimethyl-2-oxoglutarate was used at 2,5mM.

For L-BSO, the stock solution is at 225mM and was dissolve in PBS. The final concentration used for the experiment was of 40µM.

For methylester-glutathione, the stock solution is at 100mM and was dissolved in PBS. The concentrations used were 0,25mM and 0,5mM.

CellROX

In a 48 well plate, 50 000 cells were plated in 0,5mL of control or in glutamine-free condition. The plate was then incubated for an hour and a half. CellROX was then added to each well in a final concentration of 5mM. The plate was then incubated for an extra 30 minutes. The CellROX® Oxidative Stress Reagents protocol by LifeTechnologies was followed.

The plate was then spun down at 500g for 5 minutes. The media was discarded from each well and 500µL of PBS was added as to harvest the cells and transferred to 5mL round bottom polystyrene tubes.

Some wells were left unstained as control of basal fluorescence.

10 000 events of viable cells were then acquired to the FACSVerse.

Flow cytometry

Gating strategy for viability assay using AnnexinV-APC and 7-AAD-PerCP:
A total of 10 000 events were acquired.

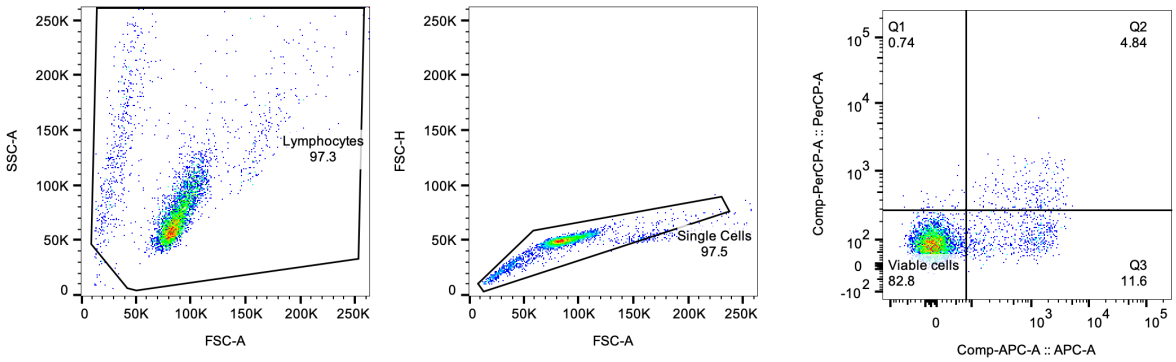

Gating strategy to quantify the level of ROS with CellROX DeepRed:
A total of 10 000 events in the first gating, corresponding to alive cells, were acquired.

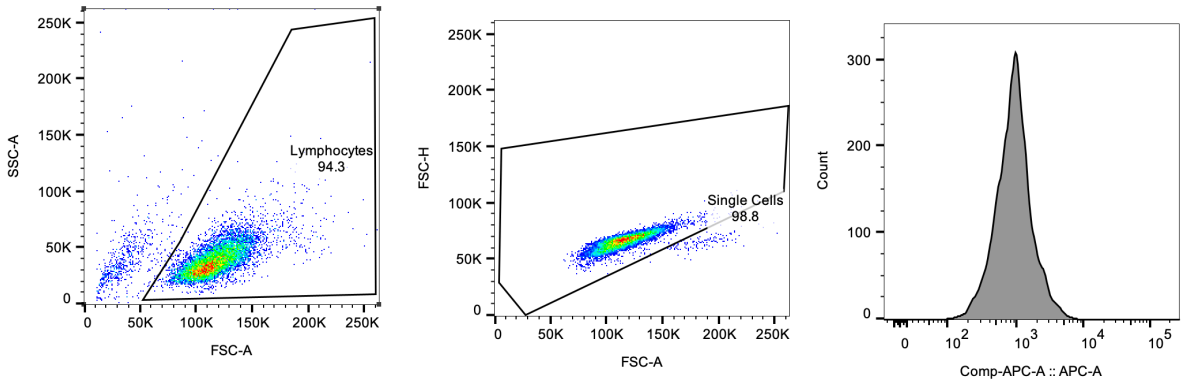

Statistical analysis

Statistical analyses were performed using GraphPad Prism (version 10.0) software. The results are expressed as the mean ± standard deviation (SD). Statistical significance was determined by Student's t test to calculate the statistical significance between two-groups, one-way analysis of variance (one-wayANOVA) to calculate the statistical significance between three groups or more with one experimental parameter, and two-way analysis of variance (two-wayANOVA) was used to calculate the statistical significance between three groups or more with two or more experimental parameters. A P value <0.05 was considered to be significantly different. (* = p-value ≤ 0.05; ** = p-value ≤ 0.01; *** = p-value ≤ 0.001; **** = p-value ≤ 0.0001)

AI

The AI ChatGPT and Gemini were used as a way to perfect the scientific style of writing of this thesis.

Material

3-hydroxy-kynurenin	27778-10, Sanbio
6-well plate	3516, Costar
7-AAD staining	420404, BioLegend
48-well plate	3548, Costar
96-well plate	3599, Costar
Agilent Seahorse XF RPMI Medium	103576-100, Agilent
Ammonium acetate	0001244153BS, Biosolve
AnnexinV-APC marker	640941, BioLegend
AnnexinV buffer	422201, BioLegend
CellROX DeepRed	C10422, Life Technologies Europe
Chloroform	J67241.K2, Life Technologies Europe
Citrate	C2404-100G, Sigma-Aldritch
dFBS	11520646, Fisher Scientific
Dimethyl-2-oxoglutarate	349631-5G, Sigma Aldritch
Dimethyl-itaconate	11303296, Fisher Scientific
Dimethyl-malonate	HY787, BioLegend
DNAse and RNAse free water	10977049, Life Technologies Europe
Ethanol	17322, Magasin Lavoisier
FACS plate	353920, Falcon
FBS	SV30160.03, Cytiva
Glucose	G7528-1KG, Sigma Aldrich
Glutamine	11510626, Fisher Scientific
Glutarate	HY-W008820, Bio-Connect
Interleukine 3 (IL3)	575508, BioLegend
Interleukine 6 (IL6)	575708, BioLegend
Isopropanol	190764-2.5L, Sigma Aldrich
Kynurenine	K8625-25MG, Sigma Aldrich
L-BSO	14484-250, Sanbio
Lysine-monohydrate chloride	62929-100F, Sigma Aldrich
Methanol	900688-1L, Sigma Aldrich
Methylester-glutathione	HY-134124, Bio-Connect
N-acetylcysteine	A9165-25G, Sigman Aldrich
PBS	12037539, Fisher Scientific
Penicillin/Streptomycin	15140122, ThermoFisher

Primer ß-actin sybrgreen	Mm.PT.58.8794492, IDT
Primer ß-actin taqman	Mm.PT.58.33540333, IDT
Primer Acly	23397720, IDT
Primer Ankh	Mm.PT.58.11270198, IDT
Primer Cpt1α	Mm.PT.58.10147164, IDT
Primer Idh2	Mm.PT.58.8461530, IDT
Primer Irg1	Mm.PT.58.42275984, IDT
Primer slc13A3	Mm.PT.58.32227093, IDT
Primer slc13A5	Mm.PT.58.16585308, IDT
Primer Slc25A1	Merck
Puromycine	ant-pr-1, InvivoGen
Pyruvate	P5280-25G, Sigma Aldrich
qPCR plastic seal	4311971, ThermoFisher
qPCR plate	4346906, ThermoFisher
RevertAid First Strand cDNA Synthesis Kit	K1622, ThermoFisher
RPMI1640	31870074, Life Technologies Europe
SCF (Stem Cell Factor)	579708, BioLegend
Slc13A5 Short hairpin (1)	TRC0000079293 5′ CGAGGGAAACACCGTTCATAT 3′
Slc13A5 Short hairpin (2)	TRC0000079296 5′ GCTCGTTCCATTGGTATCCAT 3′
Slc13A5 Short hairpin control	SHC202 5′ CAACAAGATGAAGAGCACCAA 3′
Sodium acetate	S2889-250G, Sigma Aldrich
Succinate	S9512-100G, Sigma Aldrich
SYBRGreen Master Mix	A46109, Life Technologies Europe
TaqMan Master Mix	4444964, Life Technologies Europe
Trizol	12044977, Fisher Scientific
Trypsin	25300096, Life Technologies Europe
Trypan blue	T8254, Sigma Aldrich
Tryptophan	T0254-25G, Sigma Aldrich

Results

Confirmation of the knock down of Slc13A5 by short hairpin RNAs

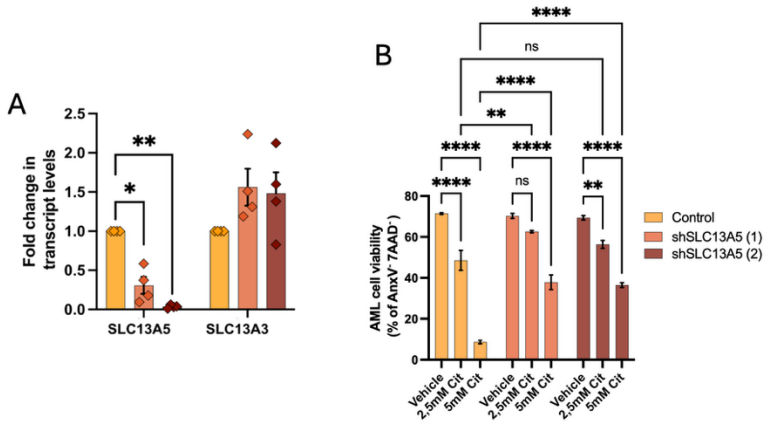

Figure 6: (A) Assessment of the control and knockdown cell lines by RT-qPCR (oneway-ANOVA); (B) Viability of control and knockdown AML cell lines assessed using annexinV and 7AAD after exposure to 2,5mM or 5mM of citrate for 24h using flow cytometry (twoway-ANOVA) (unpublished data)

To investigate the role of Slc13A5 in murine AML (mAML) cells, two MLL-AF9–driven AML cell lines were generated in which *Slc13A5* expression was knocked down using short hairpin RNAs (shRNAs). A quality control (QC) cell line transduced with a non–mammalian-targeting shRNA was used as the control. Upon revival, knockdown (KD) efficiency was evaluated using RT-qPCR to confirm maintenance of reduced *Slc13A5* expression.

As shown in figure 6A, Slc13A5 knockdown was well preserved after thawing. Interestingly, *Slc13A3* expression appeared to be slightly upregulated in Slc13A5 KD AML cells, although the increase did not reach statistical significance. This observation suggests a potential partial compensatory response by *Slc13A3* following *Slc13A5* knockdown in AML cells.

As the main metabolite transported by this solute carrier is citrate, and that AML cells express Slc13A5, the hypothesis that was initially established by the lab was that AML cells might have a higher need for exogenous citrate. However, exposing AML to increasing levels of citrate lead to an unexpected induction of apoptosis. Interestingly, the knock-down of Slc13A5 in AML cells prevents this citrate-induced toxicity, confirming that citrate is being transported by Slc13A5 in AML cells (Figure 6B).

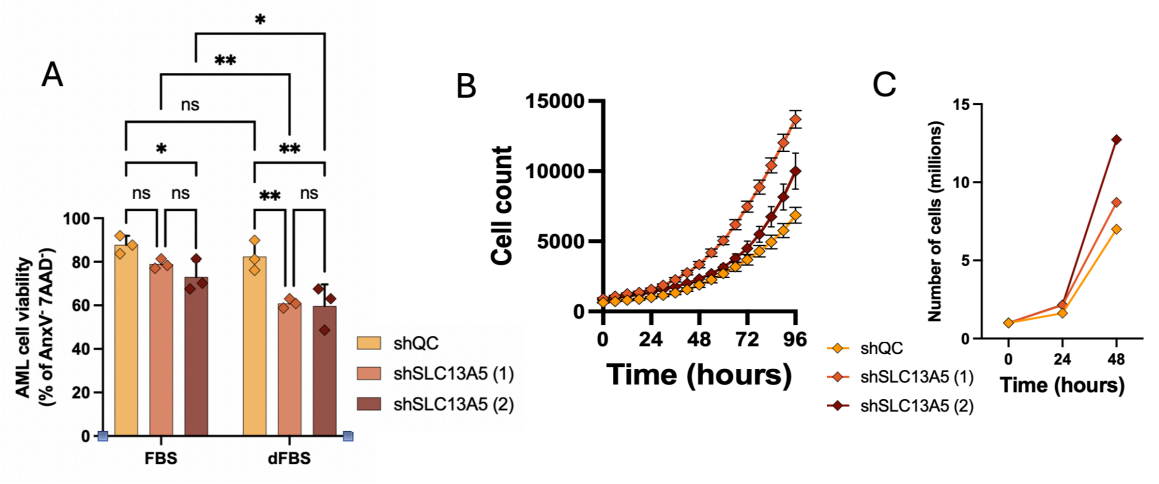

Figure 7: (A) Viability of control and knockdown AML cell lines assessed using annexinV and 7AAD after exposure to FBS or dFBS for 24h using flow cytometry (two-wayANOVA); (B) Assessment of the proliferation of the knockdown cells by ImageXpress PICO automated cell imaging system, cells were counted every 6 hours for 96 hours (pvalue < 0,0001, nonlinear regression statistical test) (unpublished data); (C) Assessment of the proliferation of the knockdown cell lines by trypan blue exclusion assay (no statistical test).

As the main metabolite that Slc13A5 transports induces a toxic effect in AML cells, this suggests that AML cells express this transporter to fulfill a need for another metabolite or metabolites. Interestingly, the viability of Slc13A5 knockdown AML cells is significantly decreased when cultured in media that was supplemented with

dialyzed serum (Figure 7A). This suggest that the lack of Slc13A5 in AML cells increases the reliance on certain metabolites that are present in the serum that we supplement our culture medium with. Intriguingly, the proliferation rate of the Slc13A5 knock down AML cells is significantly higher than the control cells (Figure 6C and 6D). As assessing using both the ImageXpress PICO Automated Cell Imagine System (Figure 6C) and automated cell counting using Cell counter Countess (ThermoFischer) during passaging using trypan blue exclusion assay (Figure 6D).

The Slc13A5 knockdown AML cell lines have a high reliance on glutamine

Given that the Slc13A5 knock down AML cells have a higher proliferative rate and seem to be more sensitive to being cultured in dFBS, we wondered in which culture conditions would Slc13A5 be important for the survival and growth of AML cells. To answer this question, we cultured the different AML cell lines in either glucose-free media and glutamine-free media and assessed their viability by flow cytometry (Figure 8A). We were unable to observe any significant change in the viability of the different cell lines compared to the control condition when cultured in glucose-free media. However, in glutamine-free media, control cells display only a slight decrease in the viability, which gets more pronounced in dFBS glutamine-free media conditions (glutamine is undetectable). This suggests that AML cells at baseline are sensitive to glutamine deprivation but can survive on low glutamine levels. Conversely, the Slc13A5 knock down AML cells display a higher sensitivity towards being cultured in glutamine-free media and show a significant induction of cell death even in the presence of 0,05-0,1mM of glutamine (in 10% FBS media) compared to the control cells. This suggests that the Slc13A5 knockdown AML cell lines have a higher need for glutamine and are more sensitive to lower glutamine

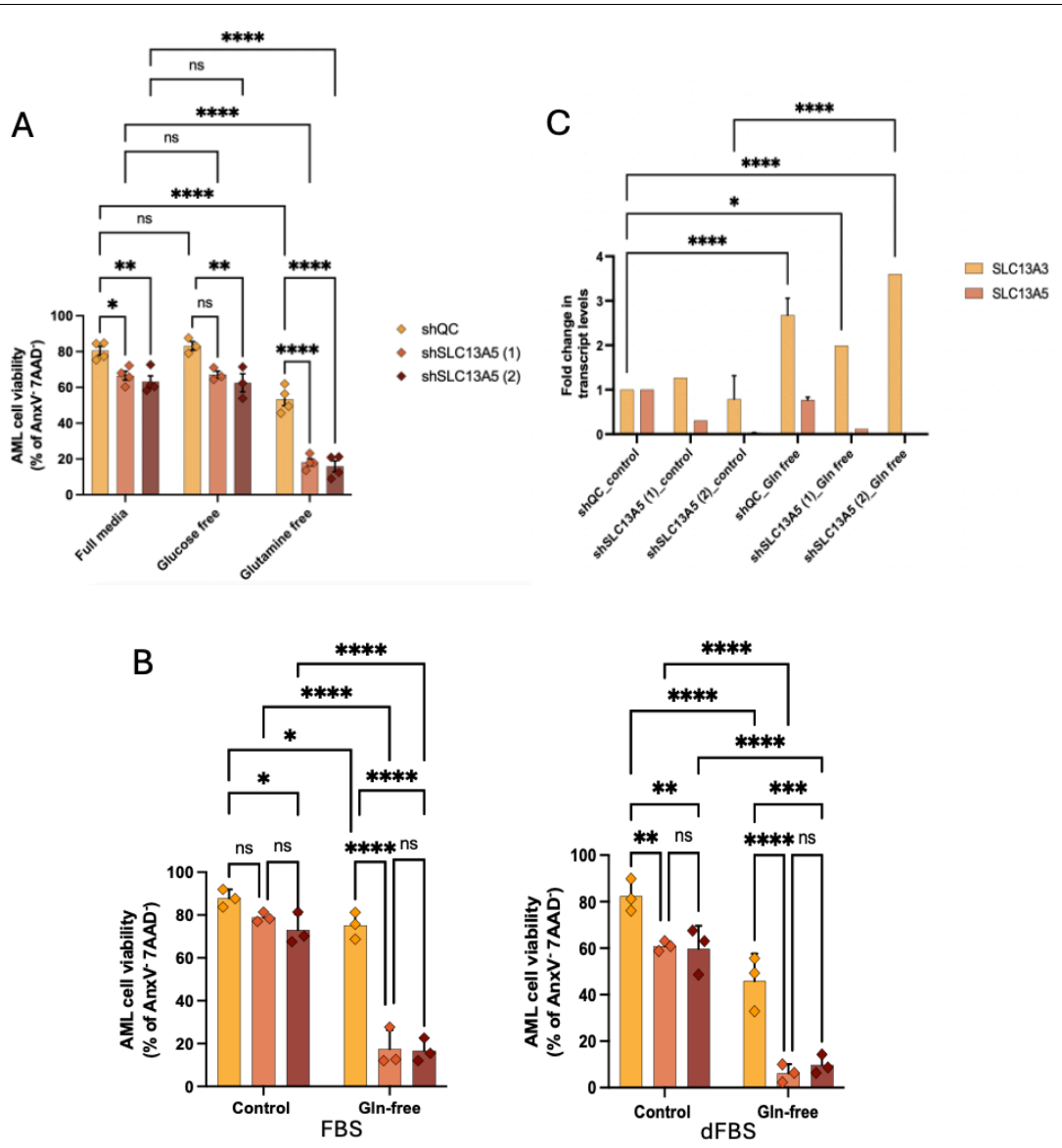

Figure 8: (A) Viability of control and knockdown AML cell lines assessed using annexinV and 7AAD after exposure to glucose-free media or glutamine-free (using FBS) media for 24h using flow cytometry (two-wayANOVA); (B) Viability of control and knockdown AML cell lines assessed using annexinV and 7AAD after exposure to glutamine-free media for 24h using flow cytometry in FBS or dFBS (two-wayANOVA); (C) Assessment of Slc13A3 and Slc13A5 mRNA expression of the control and knockdown cell lines in control and glutamine-deprived media by RT-qPCR (two-wayANOVA).

levels in the media. Interestingly, the expression of Slc13A3 and not that of Slc13A5 in significantly upregulated in control cells (as well as slc13A5 knock down AML cells) after exposure to 4h of glutamine-free media (Figure 6D). This suggest that a metabolite transported by Slc13A3 is required by AML cells when exposed to low glutamine levels as a potential compensation mechanism.

The role of glutathione/ROS in the glutamine-free induced cell death in Slc13A5 knock down AML cells

Given the increased reliance on glutamine in the Slc13A5 knock down AML cells (Figure 7B) for survival, and upregulation of Slc13A3 expression following glutamine deprivation (Figure 6D), which has been shown to facilitate the uptake of exogenous glutathione, a powerful ROS scavenger, we wondered if the glutamine deprivation induced sensitivity in Slc13A5 knock down AML cells is due to a redox dysregulation, considering the crucial role of glutamine metabolism in glutathione synthesis. Therefore, we measured the level of ROS in the AML cell lines with or without the Slc13A5 knock down (Figure 8A). We were able to see a slight yet not significant increase of total ROS levels in the Slc13A5 knockdown AML cell lines. We therefore used either N-acetylcysteine (NAC) and L-Buthionine-sulfoximine (L-BSO), as either a tool to lower ROS or increase ROS respectively in these AML cells. However, the addition of NAC did not have any protective effect in Slc13A5 knock down AML cells that were exposure to glutamine deprivation (Figure 8B). Surprisingly, the addition of NAC further sensitized control cells to glutamine deprivation (Figure 8B). Similarly, supplementing these AML cells with membrane permeable glutathione (GSH) in efforts to reverse the glutamine deprivation-induced sensitivity in Slc13A5 knock down AML cells had no significant impact on their viability (Figure 8D). Lastly, we also supplemented these cells with L-BSO, an inhibitor of γ-glutamylcysteine synthetase, the enzyme catalyzing a step of glutathione generation, and we observed no significant impact on the sensitivity towards glutamine deprivation in both control and Slc13A5 knock down AML cells (Figure 8C).

Interestingly, the levels of total ROS in Slc13A5 knock down AML cells after exposure to glutamine-free media were reverted back to normal levels, while the levels of ROS in controls cells remained the same. This suggest that glutamine-deprivation induces a depletion of ROS in Slc13A5 knock-down AML cells rather than an accumulation as initially hypothesized (Figure 8E).

As we see no impact on the glutamine deprivation sensitivity in these AML cells upon supplementing with agents that can both lower and increase basal ROS levels, we conclude that the sensitivity of Slc13A5 knock down AML cells to glutamine deprivation is not related to a redox issue.

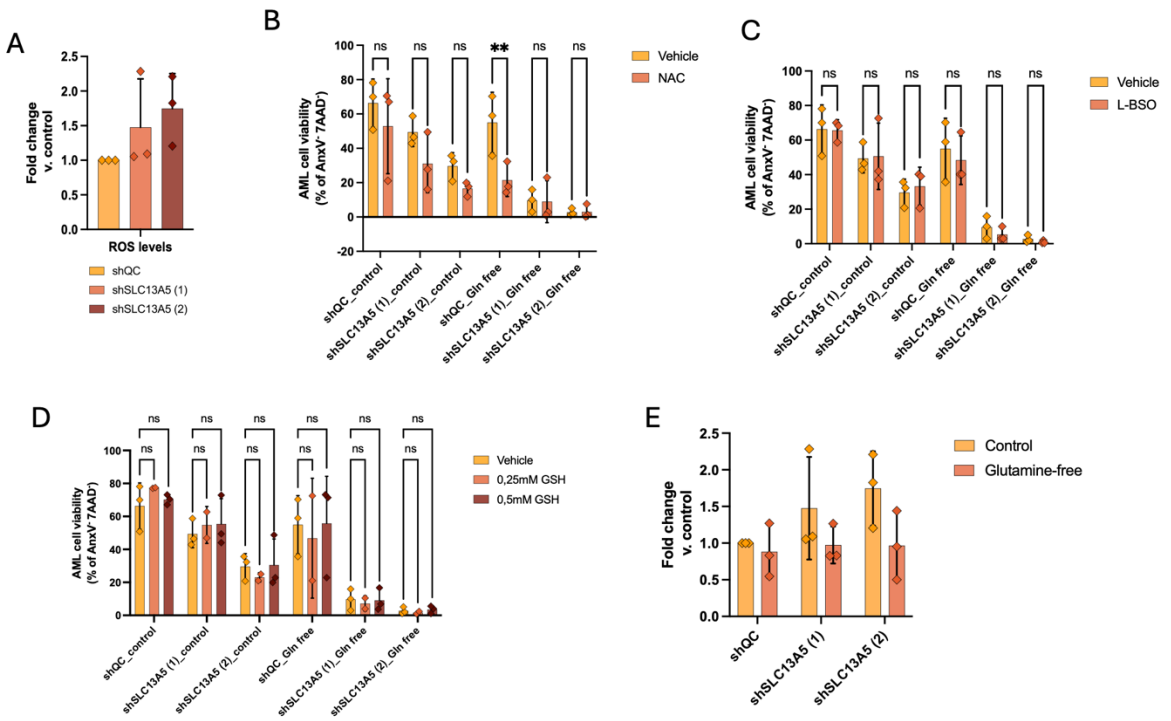

Figure 9: (A) Measurement of the ROS levels in the control and knockdown cell lines in a 48-well plate, for 2 hours (oneway-ANOVA); (B) Viability of control and knockdown AML cell lines assessed using annexinV and 7AAD after exposure to 20mM N-acetyl-cysteine (NAC) for 24h using flow cytometry in a 96well-plate (two-wayANOVA); (C) Viability of control and knockdown AML cell lines assessed using annexinV and 7AAD after exposure to 40µM L-BSO for 24h using flow cytometry in a 96well-plate (two-wayANOVA); (D) Viability of control and knockdown AML cell lines assessed using annexinV and 7AAD after exposure to 250µM or 500µM of methylester-glutathione for 24h using flow cytometry in a 96well-plate (two-wayANOVA); (E) Measurement of the ROS levels in control and knockdown cell lines in control media and in glutamine-deprived media in a 48 hours for 2 hours (two-wayANOVA).

Rescue of the viability of the Slc13A5-deficient cells in glutamine-free media

As shown in figure 2, glutamine can be metabolized in different way as to fuel different pathways. One of these is glutaminolysis and fuels the TCA cycle, by producing glutamate with glutaminase (GLS) then α-ketoglutarate with glutamate dehydrogenase (GDH). α-ketoglutarate can either be oxidized to succinate or reduced into citrate and eventually acetyl-CoA. Intriguingly, α-ketoglutarate is another metabolite that can be transported by Slc13A3 (see Figure 12). We then supplemented AML cells (with or without Slc13A5 knock down) with the membrane permeable form of α-ketoglutarate (dimethyl-2-oxoglutarate), and we were able to detect a significant reversal of the glutamine deprivation induced sensitivity in both the control cells and the Slc13A5 knock down AML cells (Figure 10). As α-ketoglutarate is one of the main metabolites that Slc13A3 transports, this rescue of the glutamine sensitivity in Slc13A5 knock down AML cells suggests that the Slc13A3 mRNA expression upregulation in AML cells upon glutamine deprivation is perhaps to compensate by taking up exogenous α-ketoglutarate.

This confirms that Slc13A5-deficient cells use glutamine as to replenish the TCA metabolites pool in the mitochondria.

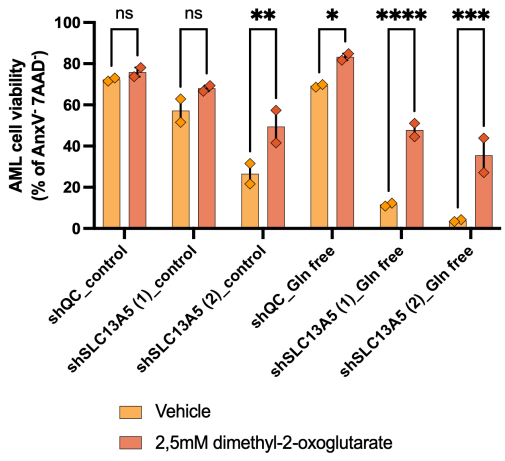

Figure 10: Viability of control and knockdown AML cell lines assessed using annexinV and 7AAD after exposure to 2,5mM of dimethyl-2-oxoglutarate for 24h using flow cytometry in a 96well-plate (two-wayANOVA)

Rescue attempts of the viability of Slc13A5 knockdown AML cells in glutamine-free media

As shown in table 1, the Slc13A5 transporter is able to import succinate and pyruvate, (metabolites that can also be imported by Slc13A3). As shown in figure 6A, we were able to see an increase of the Slc13A3 transporter in the Slc13A5 knockdown cell lines. In the different cell lines, we also observed that the Slc13A3 transporter was more expressed when the cells were cultured in glutamine-free media (Figure 8C). We started by trying to rescue the sensitivity of Slc13A5 knock down AML cells towards glutamine deprivation by adding metabolites commonly imported by both transporters such as succinate and pyruvate. For succinate, different concentrations were tested but none were able to significantly reverse the effect on the viability of these cells upon the glutamine deprivation (Figure 11A). Next, we tested supplementing with 5mM of pyruvate, there were no clear effects on the viability of these cells in glutamine-free media (Figure 11B). Another metabolite that can be transported by Slc13A3 is itaconate (a citrate-derived metabolite), however, we also saw no significant impact on the sensitivity towards glutamine deprivation in these cells (Figure 11C).

In metabolically active cells, TCA cycle intermediates are continuously sequestered via cataplerotic pathways to serve as precursors for the biosynthesis of macromolecules, including fatty acids, non-essential amino acids, and porphyrins. Glutamine plays a key role in the regulation of the TCA cycle, as it provides the primary anaplerotic flux through glutaminolysis to replenish the TCA cycle with α-ketoglutarate. It can also determine the directionality of the cycle (oxidative vs reductive), where, under normoxia, glutamine-derived α-ketoglutarate is oxidized to succinate, eventually forming oxaloacetate to facilitate ATP production. Whereas in hypoxic conditions or mitochondrial distress, the α-ketoglutarate/citrate ratio increases. This triggers Idh2 to run in reverse, carboxylating α-ketoglutarate into

isocitrate/citrate. This provides an alternative pathway generate acetyl-CoA for lipid synthesis in the cytosol other than glucose (Fendt et al., 2013).

With this in mind and given that the main metabolite that gets transported by Slc13A5 (citrate) is a source of acetyl-CoA in the cytosol, we therefore hypothesized that the glutamine deprivation-induced sensitivity in Slc13A5 knock down AML cells might be due to the lack of acetyl-CoA. Interestingly, it is also reported that Slc13A3 can import glutarate and its derivatives which can be a source of acetyl-CoA in the cytosol (Figure 11D). In addition, glutarate can be generated from lysine and tryptophan, we therefore wondered if supplementing either glutarate directly or the precursor (lysine and tryptophan) would have any effect on the glutamine deprivation-induced sensitivity in Slc13A5 knock down AML cells. We first started with supplementing with glutarate, which showed no significant increase in the viability of the cells in the glutamine-free conditions (Figure 11E). Next, we tried glutarate building blocks, lysine (Figure 11F) and tryptophan (Figure 11G), but there was no significant change. We also tried the tryptophan pathway intermediates that can eventually lead to glutarate and acetyl-CoA such as kynurenine (Figure 11H) and 3-hydroxykynurenine (Figure 11I) but there were no significant changes.

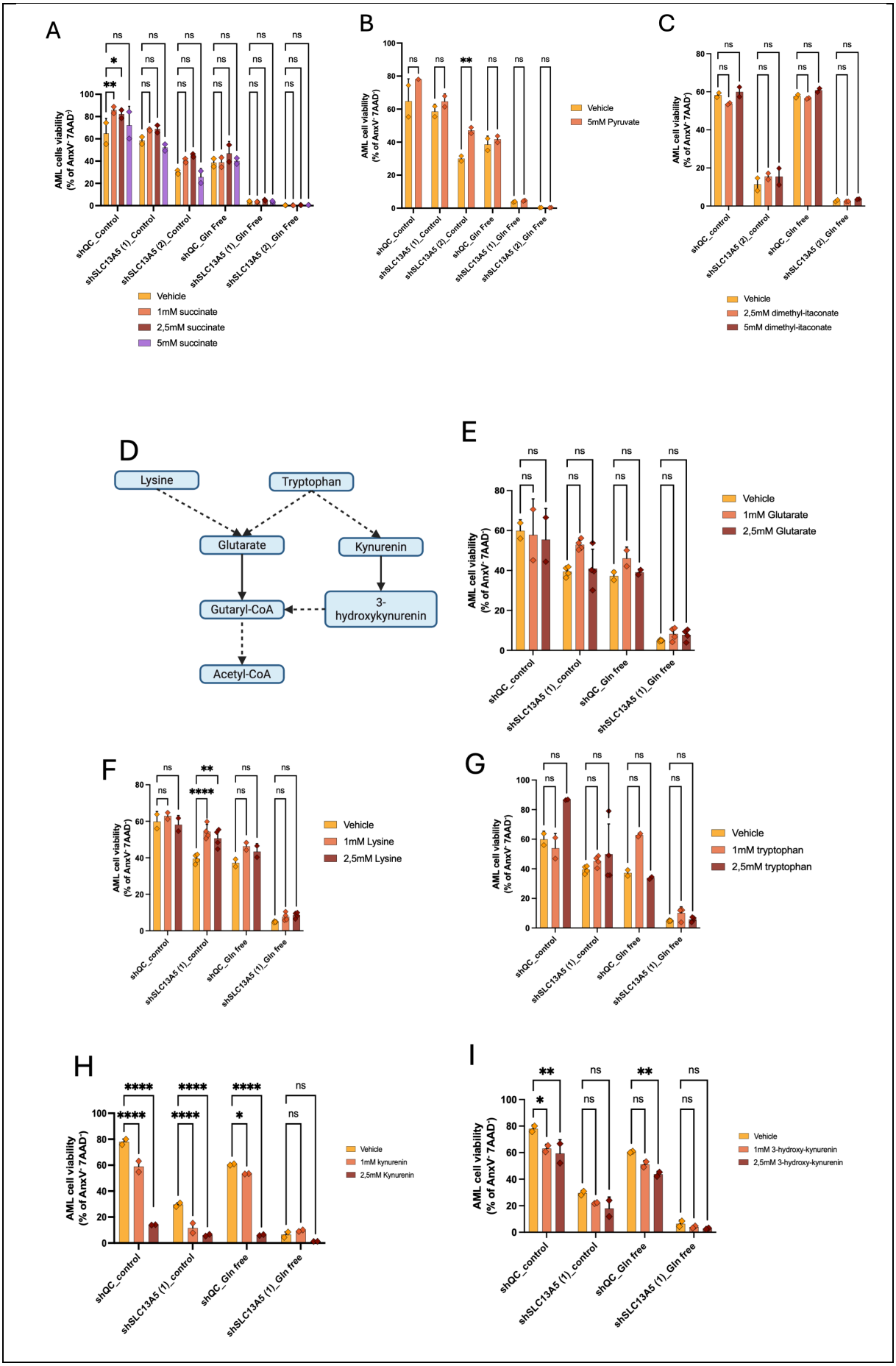
A
AML cells viability (% of AnxV⁻ 7AAD⁻)
shQC_Control
shSLC13A5 (1)_Control
shSLC13A5 (2)_Control
shQC_Gln Free
shSLC13A5 (1)_Gln Free
shSLC13A5 (2)_Gln Free
Vehicle
1mM succinate
2,5mM succinate
5mM succinate
B
AML cell viability (% of AnxV⁻ 7AAD⁻)
Vehicle
5mM Pyruvate
C
AML cell viability (% of AnxV⁻ 7AAD⁻)
shQC_control
shSLC13A5 (2)_control
shQC_Gln free
shSLC13A5 (2)_Gln free
Vehicle
2,5mM dimethyl-itaconate
5mM dimethyl-itaconate
D
Lysine
Tryptophan
Glutarate
Kynurenin
Gutaryl-CoA
3-hydroxykynurenin
Acetyl-CoA
E
AML cell viability (% of AnxV⁻ 7AAD⁻)
shQC_control
shSLC13A5 (1)_control
shQC_Gln free
shSLC13A5 (1)_Gln free
Vehicle
1mM Glutarate
2,5mM Glutarate
F
AML cell viability (% of AnxV⁻ 7AAD⁻)
shQC_control
shSLC13A5 (1)_control
shQC_Gln free
shSLC13A5 (1)_Gln free
Vehicle
1mM Lysine
2,5mM Lysine
G
AML cell viability (% of AnxV⁻ 7AAD⁻)
shQC_control
shSLC13A5 (1)_control
shQC_Gln free
shSLC13A5 (1)_Gln free
Vehicle
1mM tryptophan
2,5mM tryptophan
H
AML cell viability (% of AnxV⁻ 7AAD⁻)
shQC_control
shSLC13A5 (1)_control
shQC_Gln free
shSLC13A5 (1)_Gln free
Vehicle
1mM kynurenin
2,5mM Kynurenin
I
AML cell viability (% of AnxV⁻ 7AAD⁻)
shQC_control
shSLC13A5 (1)_control
shQC_Gln free
shSLC13A5 (1)_Gln free
Vehicle
1mM 3-hydroxy-kynurenin
2,5mM 3-hydroxy-kynurenin

Figure 11: Rescue attempts of the knockdown cells' viability in glutamine-free media: (A) Expression of Slc13A3 and Slc13A5 in glutamine-free media in shQC cell line (Student t test); (B) Viability of control and knockdown AML cell lines assessed using annexinV and 7AAD after exposure to succinate (1mM, 2,5mM and 5mM) for 24h using flow cytometry in a 96well-plate (two-wayANOVA); (C) Viability of control and knockdown AML cell lines assessed using annexinV and 7AAD after exposure to 5mM of pyruvate for 24h using flow cytometry in a 96well-plate (two-wayANOVA); (D) Viability of control and knockdown AML cell lines assessed using annexinV and 7AAD after exposure to dimethyl-itaconate (2,5mM and 5mM) for 24h using flow cytometry in a 96well-plate (two-wayANOVA); (E) Glutarate and its derivatives ; (F) Viability of control and knockdown AML cell lines assessed using annexinV and 7AAD after exposure to glutarate (1mM and 2,5mM) for 24h using flow cytometry in a 96well-plate (two-wayANOVA); (G) Viability of control and knockdown AML cell lines assessed using annexinV and 7AAD after exposure to lysine (1mM and 2,5mM) for 24h using flow cytometry in a 96well-plate (two-wayANOVA); (H) Viability of control and knockdown AML cell lines assessed using annexinV and 7AAD after exposure to tryptophan (1mM and 2,5mM) for 24h using flow cytometry in a 96well-plate (two-wayANOVA); (I) Viability of control and knockdown AML cell lines assessed using annexinV and 7AAD after exposure to kynurenine (1mM and 2,5mM) for 24h using flow cytometry in a 96well-plate (two-wayANOVA); (J) Viability of control and knockdown AML cell lines assessed using annexinV and 7AAD after exposure to 3-hydroxy-kynurenin (1mM and 2,5mM) for 24h using flow cytometry in a 96well-plate (two-wayANOVA).

To see if the protective effect of α-ketoglutarate against the glutamine deprivation-induced sensitivity in Slc13A5 knock down AML cells (figure 10) is due to it replenishing the TCA cycle by being oxidized into succinate or fueling cytosol with acetyl-CoA. We looked at different acetyl-CoA-generating genes such as ATP-dependent citrate lyase (Acly) which converts cytosolic citrate into acetyl-CoA, Slc25A1 (mitochondrial exporter of citrate) which mediate the export of citrate into the cytosol to be then used by Acly to generate acetyl-CoA, Idh2 which as mentioned above can run in reverse, carboxylating α-ketoglutarate into isocitrate/citrate in the mitochondria and

Ankh (exporter of citrate in the extracellular environment) which allows the citrate levels to remain low in the cytosol by being exported out into the microenvironment. We can see that, upon glutamine deprivation, *Acly* mRNA expression decreases in the control cells but increases in the Slc13A5 knockdown cell lines (Figure 12A). We also see that *Ankh* mRNA expression decreases only in the Slc13A5 knockdown AML cells upon glutamine deprivation. Whereas in control AML cells we conversely observe an increase upon glutamine deprivation. Interestingly we also see an

increase in *Idh2* mRNA expression in the knockdown cell line (shSlc13A5 (1) data only), which is even more pronounced when the cell line is cultured in glutamine-deprived media.

We also observed an increase in mRNA expression of the rate limiting enzyme of fatty acid oxidation Cpt1a in Slc13A5 knock-down AML cells upon glutamine deprivation more than the increase observed in control cells.

This might be a slight indication that the Slc13A5 knock-down AML cells, by being deprived of the ability to take up a source of cytosolic acetyl-CoA (citrate), upregulates glutamine reductive carboxylation to produce citrate as a source for cytosolic acetyl-CoA. We therefore tried to reverse the glutamine deprivation-induced sensitivity in Slc13A5 knock-down AML cells by supplementing with sodium acetate. While the presence of sodium acetate failed to reverse the sensitivity towards complete glutamine deprivation, it did rescue the sensitivity that we detect

when glutamine levels are lowered (1mM instead of 0mM in glutamine-free conditions) (Figure 12B). This indicates that there might be a role for acetyl-CoA in the sensitivity of Slc13A5 knock-down AML cells towards glutamine low conditions.

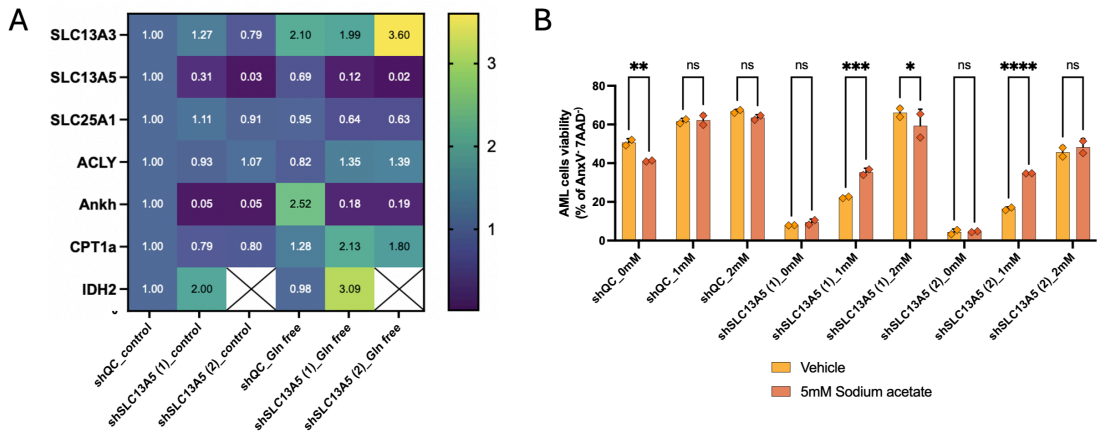

Figure 12: Effective viability rescues: (A) mRNA expression levels of acetyl-CoA related genes in SLC13A5 knockdown AML cell lines after exposure to glutamine-free media for 6hours, assessed using RT-qPCR; (B) Viability of control and knockdown AML cell lines assessed using annexinV and 7AAD after exposure to 5mM of sodium acetate for 24h using flow cytometry in a 96well-plate. For this experiment, the cells were cultured in media containing, either 0mM, 1mM or 2mM of glutamine (two-wayANOVA) (n=2, representative graph).

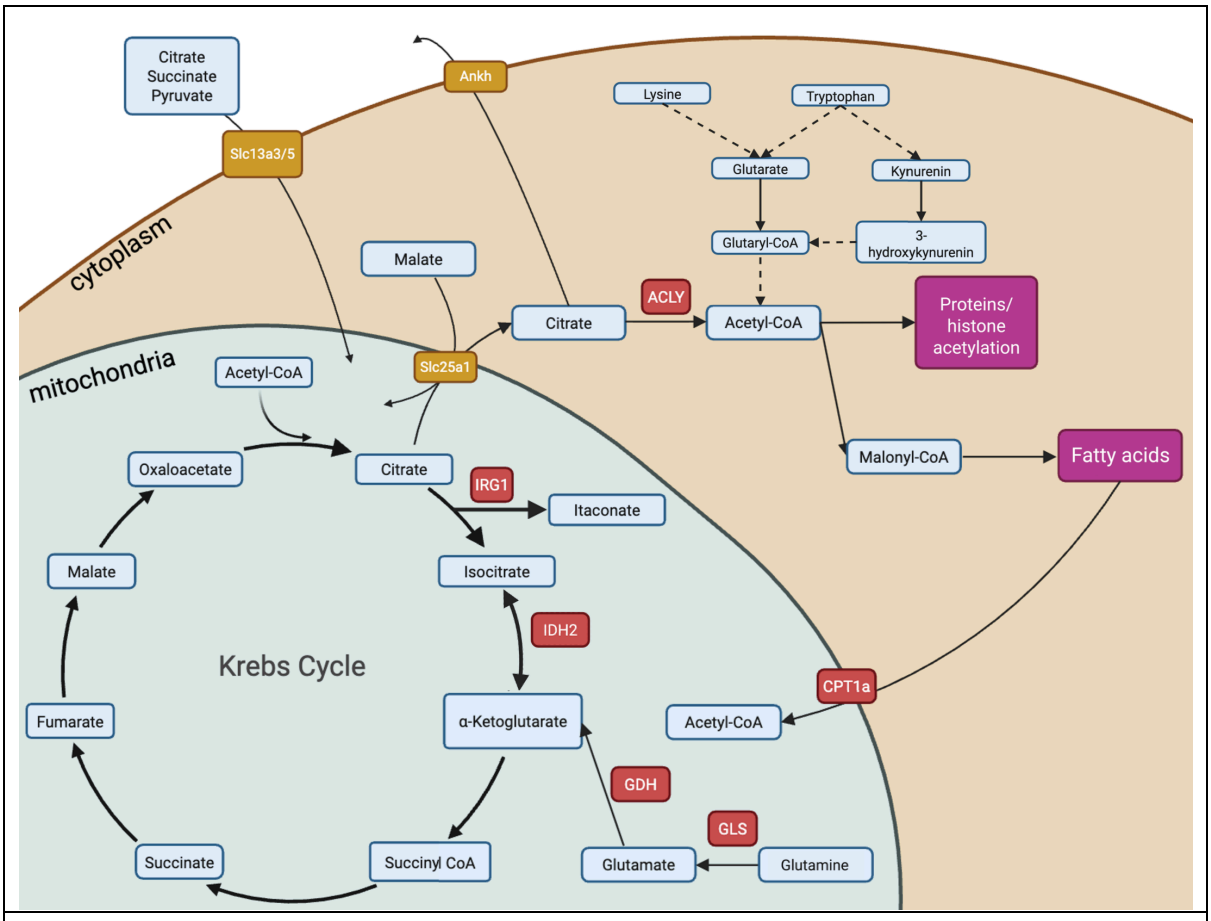

Figure 13: Schematic overview of the metabolites and pathways explored in this thesis.

Discussion

Initial characterization of Slc13A5 knockdown AML cell lines

At the beginning of this project, the functional characterization of the generated Slc13A5 AML cell lines was limited. The primary observation was an increased proliferation rate in the Slc13A5 knockdown AML cell lines, which correlated with the efficiency of Slc13A5 silencing. This phenotype was consistently observed in two independent datasets: (i) growth curves generated at the time of cell line establishment by PICO, and (ii) cell counts performed during routine passaging using trypan blue exclusion.

Given that SLC13A5 encodes a sodium-dependent transporter of TCA cycle–related metabolites, notably citrate, these findings suggested that loss of Slc13A5-mediated metabolite import induces metabolic rewiring.

Dialyzed serum reveals metabolite dependency in Slc13A5 knockdown cells

To investigate nutrient dependency, cell viability was first assessed in media supplemented with either fetal bovine serum (FBS) or dialyzed FBS (dFBS). Dialysis removes low-molecular-weight metabolites such as amino acids, sugars, vitamins, and lipids, thereby reducing experimental variability and allowing greater control over nutrient availability. Under dFBS conditions, a significant reduction in viability was observed in Slc13A5 knockdown AML cell lines compared to control cells. This result indicates that one or more metabolites depleted by dialysis are essential for the survival of Slc13A5-deficient AML cells, suggesting increased metabolic vulnerability following transporter knockdown.

Slc13A5 knockdown induces glutamine dependency

To identify the critical metabolite(s), glucose and glutamine were individually depleted from the culture medium. Glucose deprivation did not significantly affect viability in any of the cell lines, indicating that glycolytic flux is not the limiting factor under these conditions. In contrast, glutamine deprivation caused a marked reduction in viability across all AML cell lines, with a particularly strong effect in the Slc13A5 knockdown AML cells.

This observation is mechanistically significant. Under normal conditions, Slc13A5 mediates the import of extracellular citrate, which contributes to cytosolic acetyl-CoA production via ATP citrate lyase (ACLY). Loss of Slc13A5 likely reduces citrate availability, thereby limiting acetyl-CoA production. To compensate for this deficit, cells appear to increase their reliance on glutaminolysis, whereby glutamine is converted into glutamate and subsequently into α-ketoglutarate, which replenishes the TCA cycle through anaplerosis. The heightened sensitivity of knockdown cells to glutamine deprivation therefore suggests an increased dependence on glutamine-derived carbon to sustain cytosolic acetyl-CoA production.

Glutamine dependency is independent of oxidative stress

Given the known role of Slc13A3 as a transporter of glutathione, and the fact that glutathione synthesis depends on glutamine-derived glutamate, we investigated whether glutamine deprivation impaired cell viability through increased oxidative stress. Baseline ROS measurements showed a trend toward increased ROS levels in Slc13A5 knockdown AML cells. However, pharmacological modulation of ROS levels did not support a causal role for oxidative stress in the observed phenotype. Treatment with N-acetylcysteine, a ROS scavenger, unexpectedly reduced cell viability, while inhibition of glutathione synthesis with L-buthionine sulfoximine had no significant effect. Direct glutathione supplementation also failed to rescue viability. Furthermore, ROS levels were unchanged under glutamine-free conditions

in control cells, however the increased baseline levels of RNA in the Slc13A5 knock-down AML cells decreased back to normal levels upon glutamine deprivation. These findings collectively demonstrate that glutamine dependency in Slc13A5 knockdown cells is not mediated by impaired redox homeostasis.

Role of Slc13A3 in metabolic compensation

Analysis of transporter expression under glutamine-free conditions revealed a significant upregulation of Slc13A3 in control cells. This suggests a compensatory mechanism whereby Slc13A3-mediated import of alternative TCA-related metabolites partially offsets the loss of glutamine-derived carbon. In contrast, Slc13A5 knockdown cells appear unable to fully activate this compensatory pathway, further contributing to their metabolic vulnerability.

Both Slc13A3 and Slc13A5 transport metabolites that feed into mitochondrial metabolism, including citrate, succinate, pyruvate, itaconate, and glutarate. These substrates can ultimately contribute to TCA cycle flux or be converted into CoA derivatives, linking transporter activity to both anaplerosis and acetyl-CoA metabolism.

Failure of TCA intermediates to rescue viability in glutamine-free conditions

Supplementation with individual TCA cycle–related metabolites did not rescue cell viability in glutamine-free media. Succinate and pyruvate increased viability under control conditions but failed to restore survival in the absence of glutamine. Similarly, supplementation with itaconate, dimethyl itaconate, glutarate, or amino acids contributing to glutarate production (lysine and tryptophan) was ineffective.

These findings indicate that direct provision of downstream metabolites is insufficient to compensate for the loss of glutamine-derived α-ketoglutarate. This

suggests that continuous anaplerotic input via glutaminolysis, rather than the presence of individual metabolites, is required to sustain mitochondrial function in SLC13A5-deficient cells.

α-ketoglutarate rescues viability by restoring anaplerosis

To directly test the role of glutaminolysis-derived anaplerosis, cells were supplemented with dimethyl-2-oxoglutarate, a cell-permeable form of α-ketoglutarate. This treatment significantly rescued viability in glutamine-free conditions, particularly in the Slc13A5 knockdown cell lines. These results provide strong evidence that α-ketoglutarate availability is the key limiting factor underlying glutamine dependency, and that restoration of TCA cycle anaplerosis is sufficient to sustain cell survival. They also indicate that in the absence of glutamine, Slc13A5 allows AML cells to import one or more alternative anaplerotic substrates to sustain their TCA cycle activity. Whether this is citrate, or also other TCA cycle metabolites such as α-ketoglutarate or succinate, remains to be determined.

Gene expression analysis of citrate and acetyl-CoA related enzymes and transporters revealed changes consistent with intracellular citrate retention and increased acetyl-CoA production, including altered expression of *Acly*, *Slc25a1*, and *Ankh*. Given that many metabolites transported by Slc13A3 and Slc13A5 can ultimately be converted into CoA derivatives, these data suggest a broader remodeling of CoA-dependent metabolic pathways.

Supplementation with sodium acetate, a direct precursor of acetyl-CoA, was insufficient to rescue cell viability upon complete glutamine deprivation in Slc13A5 knock-down AML cells, indicating that acetyl-CoA availability alone is not limiting. However, upon partial glutamine restriction (1 mM), the addition of sodium acetate significantly restored viability in Slc13A5 knockdown AML cells, highlighting that

acetyl-CoA plays a role in the glutamine deprivation-induced sensitivity in Slc13A5 knock-down AML cells.

Consistent with this metabolic adaptation, RT-qPCR analysis showed increased expression of *Cpt1a* in Slc13A5 knock down AML cells upon glutamine deprivation, indicating enhanced fatty acid β-oxidation. This suggests that, under glutamine-limited conditions, Slc13A5 knock down AML cells attempt to maintain acetyl-CoA pools through increased fatty acid catabolism, further underscoring the central role of acetyl-CoA and TCA cycle flux in sustaining their viability upon glutamine deprivation.

Conclusion

In summary, Slc13A5 knockdown induces a metabolic state characterized by reduced citrate import, as shown in Figure 6B, increased reliance on glutaminolysis, and heightened sensitivity to disruptions in anaplerotic flux. While Slc13A3 seems to partially compensate by importing alternative metabolites, showed by the upregulation of its mRNA expression, this mechanism is insufficient under glutamine deprivation. Restoration of α-ketoglutarate levels rescues viability, demonstrating that glutamine-derived anaplerosis, rather than oxidative stress or isolated metabolite deficiency, is the primary driver of cell survival in Slc13A5-deficient cells.

Perspectives

The results presented in this study highlight a previously underappreciated role of Slc13A5 in regulating metabolic flexibility under conditions of glutamine limitation. While this work establishes a strong link between Slc13A5 knockdown, enhanced glutaminolysis, and dependence on anaplerotic flux, several important questions remain and warrant further investigation.

Further exploration of acetyl-CoA–producing pathways

Although supplementation with sodium acetate only rescues Slc13A5 AML cell viability upon exposure to lower glutamine levels, these results do not exclude a role for alternative cytosolic acetyl-CoA–producing pathways. One particularly promising candidate is N-acetylaspartate (NALA), a metabolite that can serve as a source of cytosolic acetyl-CoA following hydrolysis by aspartoacylase. Importantly, NALA has been reported as a substrate for Slc13A3 (Fujita et al., 2005), suggesting that its uptake may be enhanced in conditions where Slc13A3 expression is upregulated, such as glutamine deprivation.

Future experiments should therefore assess whether NALA supplementation can rescue AML cell viability in glutamine-free or glutamine-limited conditions, particularly in Slc13A5 knockdown AML cells. Measuring intracellular acetyl-CoA levels, histone acetylation, and lipid synthesis following glutamine deprivation in control vs Slc13A5 AML cells as well as after exposure to either acetate or NALA treatment would provide valuable insight into whether acetyl-CoA limitation contributes to the observed phenotype.

Stable isotope tracing and metabolic flux analysis

While the present study infers increased glutaminolysis and anaplerosis based on functional rescue by α-ketoglutarate, direct measurement of metabolic flux would strengthen these conclusions. Stable isotope tracing experiments using ^{13}C-labeled glutamine and ^{13}C-citrate could be employed to quantify carbon entry into the TCA cycle, citrate pools, and downstream CoA derivatives. Such approaches would clarify the relative contribution of glutamine versus other substrates to mitochondrial metabolism in Slc13A5-deficient AML cells.

Additionally, assessing whether α-ketoglutarate supplementation restores TCA cycle flux or alters citrate export and acetyl-CoA production would further define the mechanistic basis of the rescue observed in this study.

Functional dissection of Slc13A3–Slc13A5 metabolic crosstalk

The observed upregulation of Slc13A3 under glutamine-free conditions suggests functional redundancy or compensation between Slc13A3 and Slc13A5. Targeted knockdown or inhibition of Slc13A3, alone or in combination with Slc13A5 knockdown, would allow evaluation of the extent to which these transporters cooperate to maintain TCA cycle activity and acetyl-CoA availability. Such experiments could clarify whether Slc13A3 represents a secondary survival pathway upon Slc13A5 loss.

Clinical implications and therapeutic perspectives

From a translational perspective, this work provides a potential explanation for the limited efficacy of glutamine-targeting therapies in AML. Pharmacological inhibitors of glutamine metabolism, such as CB-839 (telaglenastat) or DON, aim to suppress glutaminolysis and deprive AML cells of glutamine-derived carbon. However, the present findings suggest that Slc13A5-mediated import of TCA cycle intermediates may partially bypass the requirement for glutamine, thereby sustaining

mitochondrial metabolism and limiting the therapeutic efficacy of glutamine blockade alone.

This metabolic bypass could explain why clinical attempts to inhibit glutamine metabolism using CB-839 or DON have shown limited success in certain cellular contexts (Timofeeva et al., 2023). By importing citrate or related metabolites, Slc13A5 may provide an alternative route to maintain TCA cycle flux and acetyl-CoA production despite glutamine deprivation.

Based on this rationale, a combinatorial therapeutic strategy targeting both glutamine metabolism and Slc13A5-mediated metabolite import may represent a more effective approach. Future studies should therefore evaluate whether pharmacological inhibition of Slc13A5 synergizes with CB-839 or DON to induce metabolic collapse and reduce AML cell viability. Such combination treatments could be assessed using viability assays, metabolic profiling, and in vivo models to determine their therapeutic potential.

Concluding perspective

In conclusion, this project identifies Slc13A5 as a key metabolic node that enables cellular adaptation to glutamine deprivation through enhanced anaplerosis and metabolic flexibility. By revealing how Slc13A5 supports survival under glutamine-limited conditions, this work opens new avenues for both mechanistic investigation and therapeutic intervention. Targeting Slc13A5 in combination with glutamine metabolism inhibitors may represent a promising strategy to overcome metabolic resistance mechanisms and improve the efficacy of glutamine-directed therapies in AML.

Bibliography

Bergeron, M. J., Clémençon, B., Hediger, M. A., & Markovich, D. (2013). SLC13 family of Na+-coupled di- and tri-carboxylate/sulfate transporters. *Molecular Aspects of Medicine*, *34*(2), 299-312. https://doi.org/10.1016/j.mam.2012.12.001

Cai, L., Sutter, B. M., Li, B., & Tu, B. P. (2011). Acetyl-CoA Induces Cell Growth and Proliferation by Promoting the Acetylation of Histones at Growth Genes. *Molecular cell*, *42*(4), 426-437. https://doi.org/10.1016/j.molcel.2011.05.004

Choi, B.-H., & Coloff, J. L. (2019). The Diverse Functions of Non-Essential Amino Acids in Cancer. *Cancers*, *11*(5), 675. https://doi.org/10.3390/cancers11050675

Corces, M. R., Chang, H. Y., & Majeti, R. (2017). Preleukemic Hematopoietic Stem Cells in Human Acute Myeloid Leukemia. *Frontiers in Oncology*, *7*. https://doi.org/10.3389/fonc.2017.00263

Cordes, T., Thalacker-Mercer, A. E., Pajor, A. M., Murphy, A. N., & Metallo, C. M. (2021). NaCT/SLC13A5 facilitates citrate import and metabolism under nutrient-limited conditions. *Cell reports*, *36*(11), 109701. https://doi.org/10.1016/j.celrep.2021.109701

Currie, E., Schulze, A., Zechner, R., Walther, T. C., & Farese, R. V. (2013). Cellular fatty acid metabolism and cancer. *Cell Metabolism*, *18*(2), 153-161. https://doi.org/10.1016/j.cmet.2013.05.017

Döhner, H., Weisdorf, D. J., & Bloomfield, C. D. (2015). Acute Myeloid Leukemia. *New England Journal of Medicine*, *373*(12), 1136-1152. https://doi.org/10.1056/NEJMra1406184

Farge, T., Saland, E., de Toni, F., Aroua, N., Hosseini, M., Perry, R., Bosc, C., Sugita, M., Stuani, L., Fraisse, M., Scotland, S., Larrue, C., Boutzen, H., Féliu, V., Nicolau-Travers, M.-L., Cassant-Sourdy, S., Broin, N., David, M., Serhan, N., … Sarry, J.-E. (2017).

Chemotherapy-Resistant Human Acute Myeloid Leukemia Cells Are Not Enriched for Leukemic Stem Cells but Require Oxidative Metabolism. *Cancer Discovery*, *7*(7), 716-735. https://doi.org/10.1158/2159-8290.CD-16-0441

Fendt, S.-M., Bell, E. L., Keibler, M. A., Olenchock, B. A., Mayers, J. R., Wasylenko, T. M., Vokes, N. I., Guarente, L., Vander Heiden, M. G., & Stephanopoulos, G. (2013). Reductive glutamine metabolism is a function of the α-ketoglutarate to citrate ratio in cells. *Nature communications*, *4*, 2236. https://doi.org/10.1038/ncomms3236

Fujita, T., Katsukawa, H., Yodoya, E., Wada, M., Shimada, A., Okada, N., Yamamoto, A., & Ganapathy, V. (2005). Transport characteristics of N-acetyl-l-aspartate in rat astrocytes : Involvement of sodium-coupled high-affinity carboxylate transporter NaC3/NaDC3-mediated transport system. *Journal of Neurochemistry*, *93*(3), 706-714. https://doi.org/10.1111/j.1471-4159.2005.03067.x

Haase, L., & Frezza, C. (2024). Itaconate promotes an unexpected tumor immune escape mechanism. *Cancer Cell*, *42*(12), 1988-1990. https://doi.org/10.1016/j.ccell.2024.10.011

Hanahan, D., & Weinberg, R. A. (2011). Hallmarks of Cancer : The Next Generation. *Cell*, *144*(5), 646-674. https://doi.org/10.1016/j.cell.2011.02.013

Hao, Y., Yi, Q., XiaoWu, X., WeiBo, C., GuangChen, Z., & XueMin, C. (2022). Acetyl-CoA : An interplay between metabolism and epigenetics in cancer. *Frontiers in Molecular Medicine*, *2*, 1044585. https://doi.org/10.3389/fmmed.2022.1044585

Kiyoi, H., Kawashima, N., & Ishikawa, Y. (2020). FLT3 mutations in acute myeloid leukemia : Therapeutic paradigm beyond inhibitor development. *Cancer Science*, *111*(2), 312-322. https://doi.org/10.1111/cas.14274

Kreitz, J., Schönfeld, C., Seibert, M., Stolp, V., Alshamleh, I., Oellerich, T., Steffen, B., Schwalbe, H., Schnütgen, F., Kurrle, N., & Serve, H. (2019). Metabolic Plasticity of Acute Myeloid Leukemia. *Cells*, *8*(8), 805. https://doi.org/10.3390/cells8080805

Kunchala, P., Kuravi, S., Jensen, R., McGuirk, J., & Balusu, R. (2018). When the good go bad : Mutant NPM1 in acute myeloid leukemia. *Blood Reviews*, *32*(3), 167-183. https://doi.org/10.1016/j.blre.2017.11.001

Liberti, M. V., & Locasale, J. W. (2016). The Warburg Effect : How Does it Benefit Cancer Cells? *Trends in Biochemical Sciences*, *41*(3), 211-218. https://doi.org/10.1016/j.tibs.2015.12.001

Ma, Y., Temkin, S. M., Hawkridge, A. M., Guo, C., Wang, W., Wang, X.-Y., & Fang, X. (2018). Fatty acid oxidation : An emerging facet of metabolic transformation in cancer. *Cancer letters*, *435*, 92-100. https://doi.org/10.1016/j.canlet.2018.08.006

Macečková, D., Vaňková, L., Holubová, M., Jindra, P., Klieber, R., Jandová, E., & Pitule, P. (2024). Current knowledge about FLT3 gene mutations, exploring the isoforms, and protein importance in AML. *Molecular Biology Reports*, *51*(1), 521. https://doi.org/10.1007/s11033-024-09452-2

Mesbahi, Y., Trahair, T. N., Lock, R. B., & Connerty, P. (2022). Exploring the Metabolic Landscape of AML : From Haematopoietic Stem Cells to Myeloblasts and Leukaemic Stem Cells. *Frontiers in Oncology*, *12*, 807266. https://doi.org/10.3389/fonc.2022.807266

Okuda, M. (2002). The role of nucleophosmin in centrosome duplication. *Oncogene*, *21*(40), 6170-6174. https://doi.org/10.1038/sj.onc.1205708

Panina, S. B., Pei, J., & Kirienko, N. V. (2021). Mitochondrial metabolism as a target for acute myeloid leukemia treatment. *Cancer & Metabolism*, *9*, 17. https://doi.org/10.1186/s40170-021-00253-w

RevertAid First Strand cDNA Synthesis Kit 100 Reactions | Buy Online | Thermo Scientific™. (s. d.). Consulté 7 janvier 2026, à l'adresse https://www.thermofisher.com/order/catalog/product/K1622

Robertson, K. D., Uzvolgyi, E., Liang, G., Talmadge, C., Sumegi, J., Gonzales, F. A., & Jones, P. A. (1999). The human DNA methyltransferases (DNMTs) 1, 3a and 3b : Coordinate mRNA expression in normal tissues and overexpression in tumors. *Nucleic Acids Research*, *27*(11), 2291‑2298. https://doi.org/10.1093/nar/27.11.2291

Scott, D. D., & Oeffinger, M. (2016). Nucleolin and nucleophosmin : Nucleolar proteins with multiple functions in DNA repair. *Biochemistry and Cell Biology = Biochimie Et Biologie Cellulaire*, *94*(5), 419‑432. https://doi.org/10.1139/bcb-2016-0068

Thevenon, J., Milh, M., Feillet, F., St-Onge, J., Duffourd, Y., Jugé, C., Roubertie, A., Héron, D., Mignot, C., Raffo, E., Isidor, B., Wahlen, S., Sanlaville, D., Villeneuve, N., Darmency-Stamboul, V., Toutain, A., Lefebvre, M., Chouchane, M., Huet, F., … Rivière, J.-B. (2014). Mutations in SLC13A5 cause autosomal-recessive epileptic encephalopathy with seizure onset in the first days of life. *American Journal of Human Genetics*, *95*(1), 113‑120. https://doi.org/10.1016/j.ajhg.2014.06.006

Thomas, G. E., Egan, G., García-Prat, L., Botham, A., Voisin, V., Patel, P. S., Hoff, F. W., Chin, J., Nachmias, B., Kaufmann, K. B., Khan, D. H., Hurren, R., Wang, X., Gronda, M., MacLean, N., O'Brien, C., Singh, R. P., Jones, C. L., Harding, S. M., … Schimmer, A. D. (2022). The metabolic enzyme hexokinase 2 localizes to the nucleus in AML and

normal haematopoietic stem and progenitor cells to maintain stemness. *Nature Cell Biology*, *24*(6), 872-884. https://doi.org/10.1038/s41556-022-00925-9

Timofeeva, N., Ayres, M. L., Baran, N., Santiago-O'Farrill, J. M., Bildik, G., Lu, Z., Konopleva, M., & Gandhi, V. (2023). Preclinical investigations of the efficacy of the glutaminase inhibitor CB-839 alone and in combinations in chronic lymphocytic leukemia. *Frontiers in Oncology*, *13*. https://doi.org/10.3389/fonc.2023.1161254

Tran, D. H., Kim, D., Kesavan, R., Brown, H., Dey, T., Soflaee, M. H., Vu, H. S., Tasdogan, A., Guo, J., Bezwada, D., Saad, H. A., Cai, F., Solmonson, A., Rion, H., Chabatya, R., Merchant, S., Manales, N. J., Tcheuyap, V. T., Mulkey, M., … Hoxhaj, G. (2024). De novo and Salvage Purine Synthesis Pathways Across Tissues and Tumors. *Cell*, *187*(14), 3602-3618.e20. https://doi.org/10.1016/j.cell.2024.05.011

van Gastel, N., Spinelli, J. B., Sharda, A., Schajnovitz, A., Baryawno, N., Rhee, C., Oki, T., Grace, E., Soled, H. J., Milosevic, J., Sykes, D. B., Hsu, P. P., Vander Heiden, M. G., Vidoudez, C., Trauger, S. A., Haigis, M. C., & Scadden, D. T. (2020). Induction of a Timed Metabolic Collapse to Overcome Cancer Chemoresistance. *Cell metabolism*, *32*(3), 391-403.e6. https://doi.org/10.1016/j.cmet.2020.07.009

Willems, L., Jacque, N., Jacquel, A., Neveux, N., Maciel, T. T., Lambert, M., Schmitt, A., Poulain, L., Green, A. S., Uzunov, M., Kosmider, O., Radford-Weiss, I., Moura, I. C., Auberger, P., Ifrah, N., Bardet, V., Chapuis, N., Lacombe, C., Mayeux, P., … Bouscary, D. (2013). Inhibiting glutamine uptake represents an attractive new strategy for treating acute myeloid leukemia. *Blood*, *122*(20), 3521-3532. https://doi.org/10.1182/blood-2013-03-493163

Winters, A. C., & Bernt, K. M. (2017). MLL-Rearranged Leukemias-An Update on Science and Clinical Approaches. *Frontiers in Pediatrics*, *5*, 4. https://doi.org/10.3389/fped.2017.00004

Xu, E., Ji, B., Jin, K., & Chen, Y. (2023). Branched-chain amino acids catabolism and cancer progression : Focus on therapeutic interventions. *Frontiers in Oncology*, *13*. https://doi.org/10.3389/fonc.2023.1220638

Yoo, H. C., Yu, Y. C., Sung, Y., & Han, J. M. (2020). Glutamine reliance in cell metabolism. *Experimental & Molecular Medicine*, *52*(9), 1496-1516. https://doi.org/10.1038/s12276-020-00504-8

Zehtabcheh, S., Soleimani Samarkhazan, H., Asadi, M., Zabihi, M., Parkhideh, S., & Mohammadi, M. H. (2025). Insights into KMT2A rearrangements in acute myeloid leukemia : From molecular characteristics to targeted therapies. *Biomarker Research*, *13*(1), 73. https://doi.org/10.1186/s40364-025-00786-y

Zhang, W., & Xu, J. (2017). DNA methyltransferases and their roles in tumorigenesis. *Biomarker Research*, *5*(1), 1. https://doi.org/10.1186/s40364-017-0081-z

Zhang, Z., Li, L., Wu, C., Yin, G., Zhu, P., Zhou, Y., Hong, Y., Ni, H., Qian, Z., & Wu, W.-S. (2020). Inhibition of Slug effectively targets leukemia stem cells via the Slc13a3/ROS signaling pathway. *Leukemia*, *34*(2), 380-390. https://doi.org/10.1038/s41375-019-0566-x

Zhao, W., Wang, X., Han, L., Zhang, C., Wang, C., Kong, D., Zhang, M., Xu, T., Li, G., Hu, G., Luo, J., Yee, S. W., Yang, J., Stahl, A., Chen, X., & Zhang, Y. (2024). SLC13A3 is a major effector downstream of activated β-catenin in liver cancer pathogenesis. *Nature Communications*, *15*, 7522. https://doi.org/10.1038/s41467-024-51860-2

Acute myeloid leukemia (AML) is an aggressive hematopoietic malignancy characterized by the uncontrolled proliferation of undifferentiated myeloid cells. Previous work from our laboratory has shown that bone marrow stromal cells (BMSCs) further protect AML cells by stimulating their glutamine and aspartate metabolism. Interestingly BMSCs also release TCA cycle metabolites into their microenvironment. However, whether AML cells directly utilize these BMSC-derived TCA cycle metabolites remains unknown. To determine whether AML cells are capable of taking up exogenous TCA cycle metabolites, we first assessed the expression of TCA cycle metabolite transporters. We found that AML cells express both Slc13A3 and Slc13A5. We then performed a genetic knockdown of Slc13A5 in murine AML cells and exposed them to various metabolic stress conditions. Notably, Slc13A5-deficient AML cells cultured in glutamine-free media exhibited significantly increased cell death compared to control cells, suggesting that metabolites transported via Slc13A5 are critical for AML cell survival under conditions of limited glutamine availability. Additionally, Slc13A3 expression is strongly upregulated under glutamine-free conditions, suggesting increased dependence on transporter-mediated metabolite uptake. Among potential substrates, adding α-ketoglutarate restored the viability of AML cells in glutamine-free media. α-ketoglutarate can be used to generate citrate, which is then converted into cytosolic acetyl-CoA for lipid synthesis or protein acetylation. Interestingly supplementing with acetate, partially rescued the Slc13A5-deficient cells' viability upon exposure to lower glutamine levels. This shows that the increased mortality of Slc13A5-deficient cells in glutamine-free conditions might result from a critical shortage of the acetyl-CoA pool in the cytosol. In conclusion, this project identifies Slc13A5 as a key metabolic regulator that supports AML cell survival under glutamine-deprived conditions by promoting metabolic flexibility. These findings provide new mechanistic insight into how AML cells adapt to nutrient stress and highlight Slc13A5 as a potential therapeutic target. Combining Slc13A5 inhibition with glutamine-targeted therapies may help overcome metabolic resistance and improve treatment efficacy in AML.

UNIVERSITÉ CATHOLIQUE DE LOUVAIN
Faculté de pharmacie et des sciences biomédicales
Avenue Mounier, 73 bte B1.73.06, 1200 Woluwe-Saint-Lambert, Belgique | **www.uclouvain.be/fasb**